Possibility of electroporation with microneedle-electrode array for transdermal delivery of macromolecules

2011

鄢 可書

(Keshu YAN)

Contents

Abbreviations

TDDS	transdermal drug delivery system
FD	fluorescein isothiocyanate-dextran
FL-Na	fluorescein sodium
LDH	lactate dehydrogenase
i.p.	intraperitoneal
i.c.	intracutaneous
s.c.	subcutaneous
i.m.	intramuscular
i.v.	intravenous
AUC	area under the curve
F	bioavailability
PBS	phosphate buffered saline
P	permeability coefficient
Q	cumulative permeated amount
EP	electroporation
MN	microneedle

Abstract

The usefulness of intracutaneous (*i.c.*) injection using new type of 33 gauge (G)-needles for systemic delivery of high molecular compounds was evaluated to develop the novel microneedle (MN) system for delivering macromolecules into skin. Fluorescein isothiocyanate (FITC)-dextran (FD-4; average molecular weight: 4.3 kDa) was selected as a model high molecule compound. The upper dorsal skin of hairless rat was used as an injection site. First, intravenous (*i.v.*) injection of Evans blue and *i.c.* injection of FD-4 were performed to investigate the safety of 33 G-needles. Then, the absorption rate and bioavailability of FD-4 were measured and compared after *i.c.*, subcutaneous (*s.c.*) and intramuscular (*i.m.*) injections using the 33 G-needles, while a low molecular compound, fluorescein sodium (FL-Na; 378 Da) was used for comparison.

The 33 G-needles could provide less invasive injection and more constant plasma level of FD-4 than conventional 27 G-needles. The *i.c.* injection using 33 G-needles showed higher bioavailability of FD-4 compared to *s.c.* and *i.m.* injection; on the other hand, the *i.m.* injection showed the highest bioavailability for FL. Thus, the *i.c.* injection with 33 G-needles was a promising way to increase the absorption rate and bioavailability of macromolecular drugs without severe damage to skin.

Next, a minimally invasive system was developed for the delivery of macromolecular drugs to the deep skin tissues, so called in-skin electroporation (IN-SKIN EP), using a microneedle (MN)-electrodes array. MNs were arranged to puncture the skin barrier, the stratum corneum, and were used as electrodes for EP so that a high electric field could be applied to skin tissues to promote viable skin delivery. *In vitro* skin permeation experiments showed that the IN-SKIN EP had a much higher skin penetration-enhancing effect for FD-4 than MN alone or ON-SKIN EP (conventional EP treatment), and that higher permeation was achieved by applying

a higher voltage and longer pulse width of EP.   In addition, no marked skin irritation was observed by the IN-SKIN EP, which was determined by the lactate dehydrogenase (LDH) leaching test.   These results suggest that IN-SKIN EP can be more effectively utilized as a potential skin delivery system of macromolecular drugs than MN alone and conventional ON-SKIN EP.

Finally, the MN-electrode array for IN-SKIN EP was optimized to obtain suitable skin delivery of high molecular drugs.   The MN electrodes were arranged alternately (5 anodes and 4 cathodes) or one electrode center/eight surrounding opposite electrodes (1 cathode and 8 anodes or 1 anode and 8 cathodes).   The effects of these three devices were compared on the permeation of FD-4 through hairless rat skin.   The skin surface was observed after IN-SKIN EP application by a scanning electron microscope to visualize the difference between the anode and cathode sites of skin.   In addition, skin irritation after IN-SKIN EP was evaluated by measuring the skin redness and cutaneous blood flow.   The obtained results suggested the better usefulness of the IN-SKIN EP for effectively delivering FD-4 through the skin without more severe skin irritation than conventional ON-SKIN EP.   Furthermore, the optimization of the device led to better use of the IN-SKIN EP.

Introduction

Oral administration and intravenous injections are of two major conventional ways to therapeutic delivery of drugs.   However, the former has the hepatic first-pass effect, and the latter shows markedly high plasma concentration of drugs [1, 2]. Transdermal drug delivery system (TDDS) has been paid more and more attention to overcome these problems, especially for the macromolecules such as bioactive peptides, proteins, oligonucleotides and vaccines [3-7].   However, the uppermost layer of skin, stratum corneum, limits these dosage methods only to lipophilic and low molecular drugs (less than 500 Da) [8] with high therapeutic potency. Biopharmaceuticals as explained above, such as bioactive peptides, proteins, oligonucleotides and vaccines, are rapidly growing segment in pharmaceutical therapies [3-7].   They are currently administered via parenteral routes generally due to high molecular weight, but they sometimes cause certain problems such as accidental needle sticks or pain resulting in reduced patient compliance [9].   Thus, high skin-penetration ability is necessary for developing biopharmaceutical-entrapped TDDSs as well as low molecular drug-entrapped TDDSs.

In order to overcome the high barrier function in the stratum corneum for delivering these macromolecular drugs through skin, several penetration-enhancing physical means have already been evaluated in addition to chemical enhancers to promote their skin permeation. Iontophoresis [10], electroporation (EP) [11], phonophoresis (sonophoresis) [12] and microneedles (MN) [13] are of examples. These physical means usually show higher activities or greater usefulness than chemical enhancers like low molecular alcohols and aliphatic esters [14].   Among these physical means, MN array can be utilized as an effective TDDS due to its advantage of providing a high-performance means to deliver therapeutic drugs through the skin barrier without causing marked skin damage [13, 15-18].   MN

4

arrays can be made of polymers, metal, silicone rubber, polysaccharides and so on, and create new pores in the stratum corneum barrier to enlarge the permeation pathways of several drugs [19-26]; however, such new pathways do not always result in marked skin permeation of macromolecular drugs.   Combination of the MN array with iontophoresis (MN-IP) was used to increase water flow, because electroosmosis took place through the skin from the anode to cathode in the iontophoresis system [27].   Electroosmosis may be used like a pump syringe for conventional injection (injection system consisting of a needle and pump syringe).   Another physical means, EP technology, widely used for introducing DNA and RNA into cells, biological tissues and bacteria [28, 29], is also an attracting skin-penetration enhancing method [11, 30].   EP involves the creation of tiny and transient aqueous pathways (pores) in the transcellular lipid region in the stratum corneum barrier by applying a high voltage pulse for a very short period [31].   EP application with a high-voltage electric pulse for a short period (millisecond order) results in the enhanced permeation of high molecular compounds (molecular weight of several hundreds to kilodaltons) through the skin [32-39].

For both MN and EP, in spite of their different mechanisms, enhancement of the skin permeability of drugs is a result of the creation of new permeation pathways in the stratum corneum; however, the pathways do not always persist, so that the skin barrier function is recovered immediately after the pathways close up.   TEWL (transepidermal water loss), an index of skin permeability of drugs [40], increases after the application of MN or EP and then decreases with time, which explains the recovery of skin barrier function.   To prolong the duration of new pathway (pore) openings, longer microneedles were investigated [40] and electrolytes, such as calcium salt, were applied during EP application [41] for MN and EP studies.

On the other hand, the amount and rate of macromolecule, absorbed from the skin tissues to systemic circulation, have not been clarified yet when using MN and EP technologies. Even when the macromolecules were delivered into the skin tissues, their bioavailability may be not as small molecular drugs.

In Chapter 1 of this study, a model drug, fluorescein isothiocyanate (FITC)-dextran (FD-4; average molecular weight: 4.3 kDa), was intracutaneously, subcutaneously and intramuscularly injected by 33G-needles, and the amount and rate of FD-4 systemically absorbed following the intracutaneous (*i.c.*), subcutaneous (*s.c.*) and intramuscular (*i.m.*) injections by 33G-needles were evaluated to demonstrate the feasibility of transdermal delivery of macromolecules. In Chapter 2, the synergic action of MN and EP was considered to further increase the skin permeation and bioavailability of FD-4 to achieve a longer duration of pore opening for higher skin permeation of the macromolecule. Then, the newly combination of MN and EP, so-called in-skin electroporation (IN-SKIN EP), was developed to combine the advantages of MN and EP. New MN arrays were designed and combined with EP to enhance the permeability of hydrophilic FD-4 through the stratum corneum. The influence of this EP system on the distribution of drugs in skin was also studied. Besides, in Chapter 3, the respective contribution of the cathode and the anode position was studied to the skin permeability of the drug. Then, the specific arrangement of MN as electrodes was discussed in detail. The *in vivo* assessment of this EP system was also conducted.

Chapter 1
Usefulness of intracutaneous injection by 33 gauge-needles for systemic delivery of high molecular compounds

1.1. Introduction

Intracutaneous (*i.c.*) injection is always utilized for monitoring the abnormal response of drugs [42] or immunization [43-45], as the skin is an important immune organ. It is also applied in anesthesiology study [46, 47]. Transdermal drug delivery system (TDDS) has been paid great attention aiming for avoidance of gastrointestinal side effect and hepatic first-pass effects as well as an increase in patient compliance. Besides the conventional chemical and physical approaches to increase skin permeation of drugs [48, 49], *i.c.* injection itself can be used to provide the higher bioavailability of therapeutic quantities by evading the barrier function in the stratum corneum. The *i.c.* injection using MN or needle-free injection has already been studied as a new promising method to transdermally deliver therapeutic drugs [50-53].

Since abundant blood capillaries are existed in the dermis, however, such blood capillaries may be damaged by needle intervention into skin. Big needles from a gauge (G) size of 23 to 27 G are mainly used for the subcutaneous (*s.c.*) and intramuscular (*i.m.*) injection in patients. Reduction of gauge size of needle and change from *s.c.* or *i.m.* to *i.c.* injection are expected to reduce skin damage by injection. At the same time, injection pain may be reduced by using small needles. On the other hand, diffusion rate of drugs through the skin tissues is affected by their molecular weights [52]. Generally, macromolecules diffuse across tissues very slowly [54, 55]. Thus, additional study on the drug distribution and absorption in skin must be necessary especially for designing TDDS containing macromolecules.

In the present study, a very small needle, newly developed 33 G-needle (NANOPASS[®] 33, Terumo Corp., Tokyo, Japan), was used.   FD-4 was selected as a model drug, whereas fluorescein sodium (FL-Na; 378 Da) was chosen for comparison. The bioavailability (F) and peak drug concentration (C_{max}) in plasma of FD-4 and FL were obtained after *i.c.* injection using 33 G-needles and compared with those after *s.c.* and *i.m.* injection as well as using conventional 27 G-needles.   Since the histological structure can affect the drug absorption rate from site of injection [56-60], obtained pharmacokinetics results were evaluated from a histological viewpoint.

1.2. Materials and methods

1.2.1. Materials

FD-4 and FL-Na were purchased from Sigma Aldrich (St. Louis, MO, U.S.A.). Other chemicals and reagents were of analytical grade and used without further purification.

1.2.2. Injection needles

Two sizes of injection needles, 27 G-needles (outside diameter, 0.4 mm) and 33 G-needles (outside diameter, 0.2 mm) for *i.c.* injection, were purchased from Terumo Corporation (Tokyo, Japan) (Fig. 1).
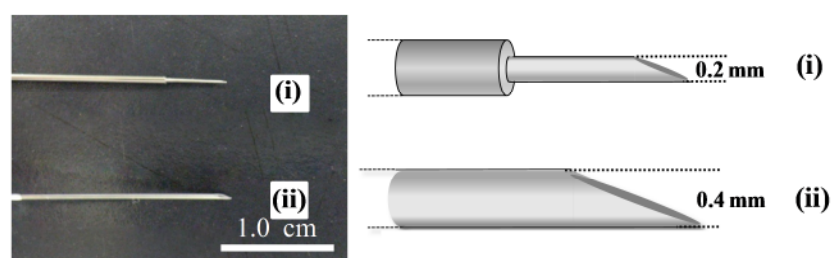

Fig. 1.   Photograph (a) and illustration (b) of 33 G (i) and 27 G (ii) injection needles.

1.2.3. Experimental animals

Male hairless rats (WBM/ILA-Ht, 7–9 weeks old) of approximately 280-300 g were supplied either by the Life Science Research Center, Josai University (Sakado, Saitama, Japan) or Ishikawa Experimental Animal Laboratory (Fukaya, Saitama, Japan). They were kept at room temperature (25 ± 2°C) with a 12 h light–dark cycle (07:00–19:00 h). The rats were anesthetized with urethane (1.0 g/kg, *i.p.*) and the hair on their abdomen was shaved. Their body temperature was maintained at 36.5 ± 0.5 °C throughout the experiments with a piece of electric carpet (Panasonic Corp., Osaka, Japan). All animal experiments were authorized by the ethics committee of Josai University (Sakado, Saitama, Japan) and conducted in according to principles of the guidelines for animal experiments at Josai University.

1.2.4. Intravenous injection (i.v.) of Evans blue with different needles

Evans blue (1.0 mg/mL, 0.2mL) was injected into the jugular vein of rats, and 150 mM NaCl (40 µL) was intracutaneously injected with a 27 and 33 G-needles in different sites of the upper dorsal skin. Then the appearance of injection sites was compared to evaluate the change in the cutaneous blood vessels.

1.2.5. I.c. injection of FD-4 with different needles

FD-4 (1.0 mg/mL, 40 µL) was intracutaneously loaded with a 27 or 33 G-needles into the abdomen of anesthetized rats. After injection, blood samples were periodically collected from the jugular vein and centrifuged (18,800×g, 5 min, 4 °C) to obtain plasma. The samples were frozen and stored at −20 °C until analysis.

1.2.6. I.v. injection of FD-4/FL-Na

FD-4 or FL-Na (1.0 mg/mL, 40 µL) was injected with 27 G-needles into the jugular vein of rats, and blood samples were collected from the contralateral jugular vein at predetermined times.   The preparation of blood samples was the same as in *1.2.5.*

1.2.7. I.c., s.c. and i.m. injection of FD-4/FL-Na with 33 G needles

FD-4 or FL-Na (1.0 mg/mL, 40 µL) was loaded by *i.c.*, *s.c.* and *i.m.* injections with a 33 G-needles into the abdomen site of anesthetized rats.   In the *i.c.* and *s.c.* injections, the drug solution was loaded at the approximately same position in skin without fixing the depth from the skin surface.   In the *i.m.* injection, Evans blue was firstly injected to confirm the site of drug delivery and the site of injection was dissected and observed until reproducible results were obtained.   The preparation of blood samples was the same as in *1.2.5.*

1.2.8. Assay

Both of FD-4 and FL in plasma samples were measured at an excitation wavelength of 495 nm and an emission wavelength of 515 nm using a spectrophotofluorometer (RF-5300 PC, Shimadzu, Kyoto, Japan).

1.2.9. Pharmacokinetic analysis

The systemic absorption rate and bioavailability of FD-4 and FL were determined according to the FDA guideline [61].   Partial bioavailability from zero to T_{max} ($F_{0-T_{max}}$) was used as an index of absorption rate, and bioavailability in 8 h ($F_{0-8 h}$) was determined for an index of whole absorption amount. C_{max} was also evaluated

as an index of absorption rate and retard absorption.

1.2.10. Statistical analysis

Statistical analysis was performed using Student's t-test and analysis of variance (ANOVA). Probability less than 0.05 was considered to be significant.

1.3. Results and discussion

1.3.1. Appearance of injection site

First, *i.c.* injection of 150 mM NaCl was done using 27 G- or 33 G-needles in rats. Then Evans blue was intravenously injected. When the skin tissue is damaged by needles, Evans blue is leached from the systemic circulation into the skin tissues [62]. The 33 G-needle caused less damage than the 27 G-needle, clearly evaluated as shown in Fig. 2.

1.3.2. Systemic disposition of FD-4 after i.c. injection using different needles

Figure 3 shows the time course of plasma concentration of FD-4 after *i.c.* injection with 27 G- and 33 G-needles into the abdomen of rats. The 27 G-needle injection showed a higher maximum plasma concentration (0.398 ± 0.015 μg/mL) at 60 min, and lower value (0.025 ± 0.005 μg/mL) at 480 min than 33 G-needle injection
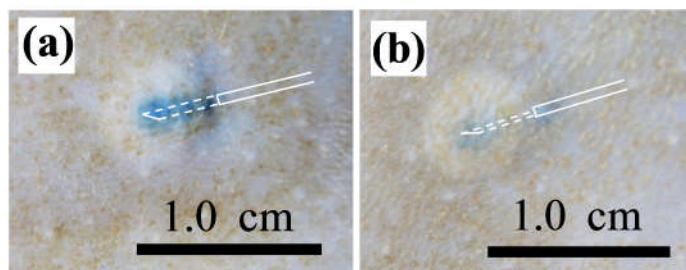

Fig. 2. Influence of *i.c.* injection using 27 G-needle (a) and 33 G-needle (b) on the leaching of Evans blue from the cutaneous capillaries.
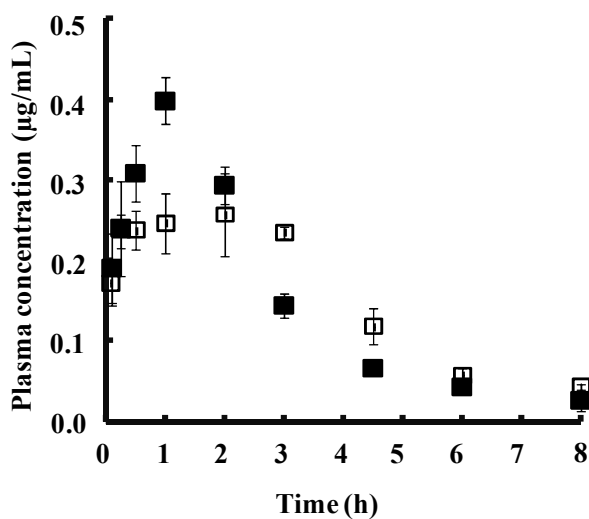
Fig. 3. Time course of plasma concentration of FD-4 after *i.c.* injection with 27 and 33 G-needle in the abdomen of rats. Symbols: ■ 27 G, □ 33 G.

(0.047 ± 0.003 µg/mL). The 33 G-needle injection showed more steady plasma profile of FD-4 over 8 h than 27 G-needle injection. No obvious peak was observed in the profile, in spite of the plateau concentration (about 0.25 µg/mL) lasting from 0.5 to 3 h.

These data were also analyzed from a pharmacokinetic viewpoint. Figure 4 shows the extent of bioavailability (F) and C_{max}. Even though $F_{0-8 h}$ for the injection with the 33 G-needle (73.2 ± 6.5%) was not significantly different from that with the 27 G-needle (77.2 ± 0.3%), the $F_{0-T_{max}}$ (13.6 ± 0.2%) and C_{max} (0.24 ± 0.04 µg/mL) for 33 G-needle injection were less than those for the 27 G-needle injection ($F_{0-T_{max}}$: 17.7 ± 0.2% and C_{max}: 0.39 ± 0.02 µg/mL). The external diameter of the 33 G-needle is half of the 27 G-needle, so that the 33 G-needle may cause less damage in blood capillaries than the 27 G-needle. Thus, the *i.c.* injection with 33 G-needle could provide stable plasma concentration than the 27 G-needle.
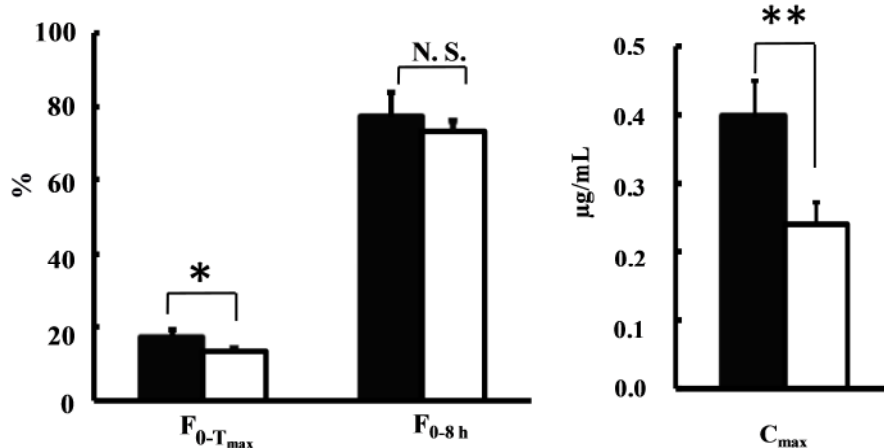
Fig. 4.   Bioavailability and C_{max} of FD-4 after *i.c.* injection with 27 and 33 G-needle in the abdomen of rats.   Symbols: ■ 27 G, □ 33 G. (*, $P < 0.05$; **, $P < 0.01$; N.S., $P>0.05$)

1.3.3. Systemic disposition of FD-4 and FL after injection with a 33 G-needle into different sites

1.3.3.1. Pharmacokinetics of FD-4 and FL after i.v. injection

Figure 5 shows the time course of plasma concentration of FD-4 and FL after *i.v.* injection.   The obtained drug concentrations in plasma were fitted to the two-compartment model by a nonlinear least-square method (software, MULTI, Yamaoka et al., 1981, algorithm, Damping Gauss–Newton method).
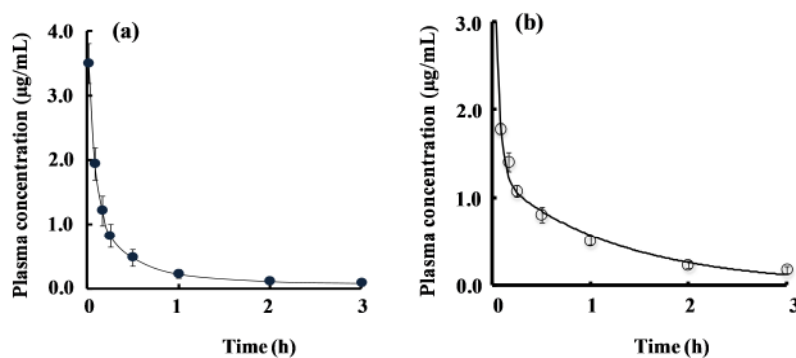
Fig. 5.   Time course of plasma concentration of FD-4 (a) and FL (b) after *i.v.* injection.

13

	FD-4	FL
A (µg/mL)	3.599 ± 0.176	3.807 ± 0.485
α (min^{-1})	0.140 ± 0.020	0.340 ± 0.034
B (µg/mL)	0.565 ± 0.030	1.259 ± 0.094
β (min^{-1})	0.010 ± 0.006	0.013 ± 0.001
$AUC_{0-\infty}$ (µg · min · mL^{-1})	97.570 ± 25.546	106.500 ± 13.525

Table 1 shows calculated pharmacokinetic parameters (A, B, α, β and $AUC_{0-\infty}$) for FD-4 and FL. The $AUC_{0-\infty}$ was used for the calculation of bioavailability after *i.c.*, *s.c.* and *i.m.* injection.

1.3.3.2. Pharmacokinetics of FD-4 after i.c., s.c. and i.m. injection

Figure 6 illustrates the time course of plasma concentration of FD-4 after *i.c.*, *s.c.* and *i.m.* injection with a 33 G-needle in the abdomen of rats. The data for *i.c.* injection, which was displayed in dashed symbols, was the same to the data for 33 G-needle injection in Fig. 4, showed the highest concentrations in the whole process.

Fig. 6. Time course of plasma concentration of FD-4 after *i.c./s.c./i.m.* injection with 33 G-needle in the abdomen of rats. *I.c.* injection data are the same as in Fig. 3. Symbols: ⊡ *i.c.*, □ *s.c.*, ▲ *i.m.*
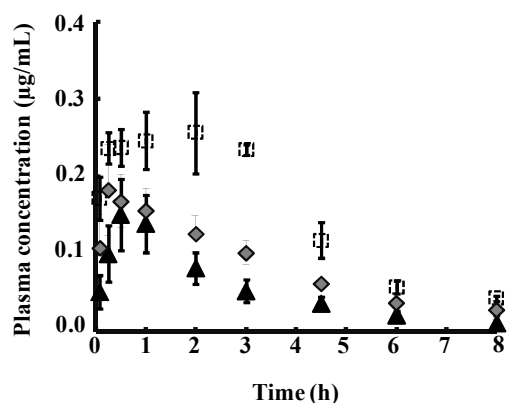
Fig. 7. Bioavailability and C_{max} of FD-4 after *i.c./s.c./i.m.* injection with 33 G-needle in the abdomen of rats. *I.c.* injection data are the same as in Fig. 4. Symbols: ▫ *i.c.*, ▪ *s.c.*, ■ *i.m.* (*, $P < 0.05$; **, $P < 0.01$)

Figure 7 summarizes the bioavailability and C_{max} of FD-4 calculated by the data in Fig. 6. *I.c.* injection showed significantly higher $F_{0-T_{max}}$ (13.3 ± 1.3%), $F_{0-8 h}$ (65.4 ± 6.4%) and C_{max} (0.25 ± 0.05 µg/mL) than *s.c.* injection ($F_{0-T_{max}}$: 7.5 ± 0.2%, $F_{0-8 h}$: 37.6 ± 6.4% and C_{max}: 0.18 ± 0.07 µg/mL) or *i.m.* injection ($F_{0-T_{max}}$: 4.4 ± 3.0%, $F_{0-8 h}$: 25.5 ± 8.1% and C_{max}: 0.16 ± 0.06 µg/mL) ($P<0.01$). In addition, these parameters after *s.c.* injection were higher than those after *i.m.* injection ($P<0.05$). The rank order of absorption amount of FD-4 was *i.c.* injection > *s.c.* injection > *i.m.* injection.

1.3.3.3. Pharmacokinetics of FL after i.c., s.c. and i.m. injection

Figure 8 shows the time course of plasma concentration of FL after *i.c.*, *s.c.* and *i.m.* injection with a 33 G-needle in the abdomen of rats. Since the molecular weight of FL is much lower than that of FD-4, the absorption of FL rate from the subcutaneous tissue and muscle was much faster than that of FD-4. Especially, absorption rate of FL was so fast after *i.m.* injection, where the T_{max} appeared 5 min after injection, much earlier than *i.m.* injection of FD-4.

15

Figure 9 shows that $F_{0-T_{max}}$ (38.3 ± 1.0%), $F_{0-8\,h}$ (92.1 ± 4.9%) and C_{max} (1.24 ± 0.09 μg/mL) of FL after *i.m.* injection were higher than those after *i.c.* ($F_{0-T_{max}}$: 17.3 ± 1.1%; $F_{0-8\,h}$: 50.9 ± 8.6%; C_{max}: 0.37 ± 0.05 μg/mL) or *s.c.* ($F_{0-T_{max}}$: 13.4 ± 0.4%; $F_{0-8\,h}$: 43.0 ± 7.5%; C_{max}: 0.32 ± 0.02 μg/mL) injection (*P*<0.01), the rank order of absorption amount was *i.m.* injection > *i.c.* injection > *s.c.* injection.

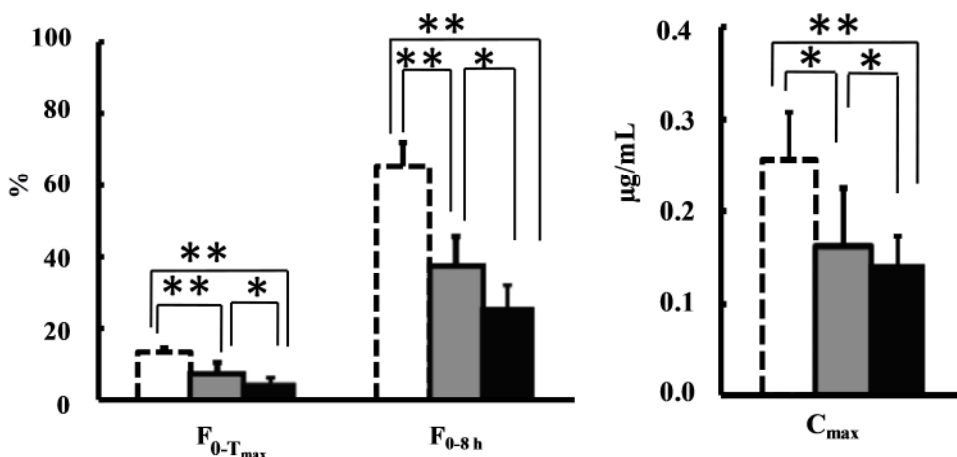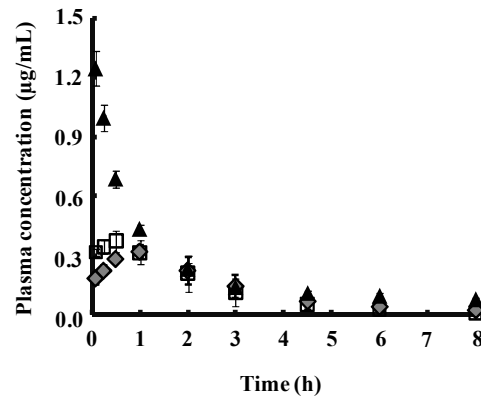Fig. 8.　Time course of plasma concentration of FL after *i.c./s.c./i.m.* injection with 33 G-needle in the abdomen of rats. Symbols: □ *i.c.*, □ *s.c.*, ▲ *i.m.*
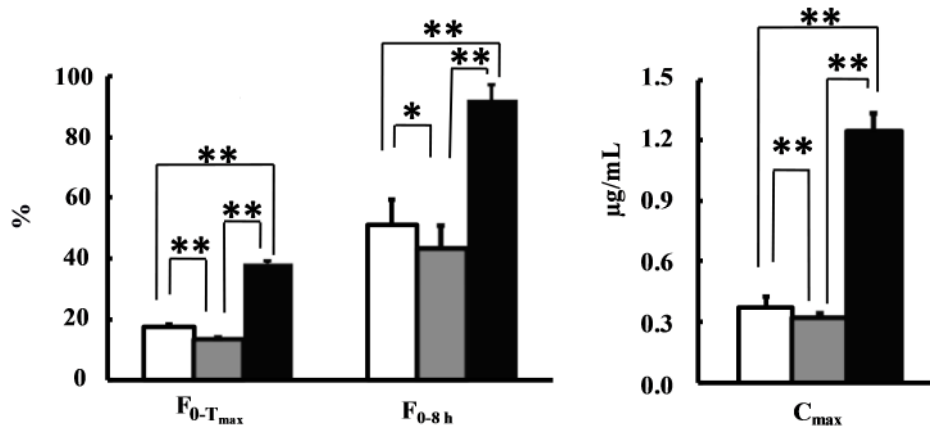

Fig. 9.　Bioavailability and C_{max} of FL after *i.c./s.c./i.m.* injection with 33 G -needle in the abdomen of rats.　Symbols: □ *i.c.*, ■ *s.c.*, ■ *i.m.* (*, *P* < 0.05; **, *P* < 0.01; N.S., *P*>0.05)

16

1.4. Discussion

Blood capillaries abundantly distribute in the skin, subcutis and muscle, but capillary density and blood flow are different in these different sites [63]. When the drug molecule is absorbed from these local tissues into the circulation after injection, the absorption process can be considered to be two steps: (1) the drug molecules enter blood capillaries from the topical tissues, where the absorption rate (entering rate) is limited by the capillary density and intercapillary connections; and (2) the drug molecules are transferred to the systemic circulation system from the local blood capillaries, where the absorption rate is limited by blood flow of capillaries.

Based on the hypothesis as above, the capillary wall acts the rate-limiting barrier after injection of a macromolecule, FD-4. More capillaries are found in the subcutis than in the skin and muscle [63]. Intercapillary connections and spatial structure of capillaries are considered as the other impact factors for drug absorption. The capillaries distribute as a serried reticulation, and the capillaries present the typical spatial arrangement in the subcutis and skin. On the other hand, the capillaries are straightened in the longitudinal axis of the muscle fibers. Furthermore, rare intercapillary connection and slight capillary tortuosity are found. Thus, the absorption rate from the subcutis is estimated to be the highest among those from skin, subcutis and muscle, and drugs in the muscle are estimated to be absorbed most slowly. The present results, however, indicated that the *i.c.* injection showed the highest absorption amount and rate of a high molecular compound, not in the *s.c.* injection. It might be attributable to poorer elasticity of skin tissue and stratum corneum, and the increase in the inner pressure of the skin tissues, which could accelerate the drug diffusing into dermis, subcutaneous tissue and muscle. Thus, the rank order in the absorption amount and rate of FD-4 was *i.c.* > *s.c.* > *i.m.* injection.

FL was distributed rapidly into capillaries, because the capillary wall is not a big barrier for the FL permeation.   The absorption rate of FL into the circulation system was rather limited by the blood flow of local capillary.   The blood flow velocity of these tissues is found to be in the order of muscle > skin > subcutis [63], which corresponds to the presently observed results after injection of FL-Na.

1.5. Chapter conclusion

The present analysis as above indicated that the new type of 33 G-needles could provide less invasive injection and more steady plasma drug level.   *I.c.* injection showed a higher absorption than *s.c.* and *i.m.* injection for a macromolecule, FD-4. The *i.c.* injection was a promising way to increase the safety and bioavailability of macromolecular drugs with low skin irritation.   Furthermore, it was also confirmed that the skin could be an effective application site for macromolecular drugs.   Thus, the delivery of macromolecular drug from skin, such as microneedle system, is clearly beneficial and feasible.

Chapter 2

Transdermal drug delivery by in-skin electroporation with microneedle array

2.1. Introduction

Several physical means have been evaluated in addition to chemical enhancers to overcome the formidable barrier of the stratum corneum and promote the skin permeation of drugs. According to the advantage of MN and EP, an electrically active MN array was produced as a device for the present IN-SKIN EP. Each MN could serve as a microelectrode for EP, which forms an electric field inside the skin barrier. After the IN-SKIN EP application, drugs are administered to the skin surface to be delivered into the deeper skin tissues. This system is different from conventional EP (ON-SKIN EP), where electrodes are applied just on the skin surface. IN-SKIN EP may facilitate the delivery of high molecular and hydrophilic compounds to deep skin tissues. Furthermore, it affects only a shallow region of skin, not a deep skin tissue by the MN-electrode array; thus, IN-SKIN EP probably increases skin permeability but with low skin irritation.

In this chapter, skin punctures made by MN were observed by a scanning electron microscopy (SEM) and a confocal laser scanning microscopy (CLSM). The effects of IN-SKIN EP were investigated on the intradermal distribution and skin permeation of FD-4 by *in vitro* skin permeation experiments. In addition, a lactate dehydrogenase (LDH) leakage assay was carried out to evaluate skin damage after the IN-SKIN EP pretreatment.

2.2. Materials and methods

2.2.1. Chemicals and animals

The chemicals and animals used in this experiment were the same as described in

the previous chapter.　The hairless rats were anesthetized by peritoneal injection of sodium pentobarbital (50 mg/kg) and hair on the abdomen was carefully shaved using an electric clipper.　Abdominal full-thickness skin was excised and adhering fat and connective tissues were carefully eliminated with a ring-ended forceps.　The excised skin was confirmed to have no damage, and was immediately used for the experiment. All animal experiments were authorized by the ethics committee of Josai University (Sakado, Saitama, Japan) and conducted in according to principles of the guidelines for animal experiments at Josai University.

2.2.2. Application of IN-SKIN EP using an MN-electrode array

The MN-electrode array for IN-SKIN EP application, shown in Fig. 10, was prepared by modification of our previous method [27].　It was assembled using 9 acupuncture needles (Haruhari, 1.5 mm; Taiho Medical Products Co., Ltd., Hiroshima,
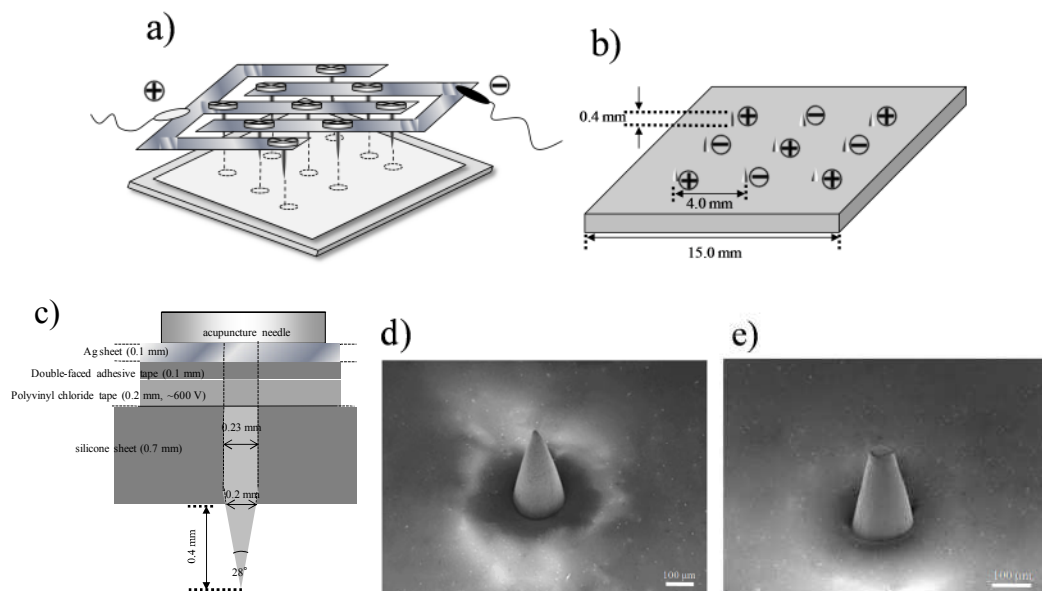

Fig. 10.　Schematic illustration of MN electrode-array made by acupuncture needles.　a) Top view, b) Back view, c) Side view, d) Microphotograph of needle tip, e) Microphotograph of obtuse needle tip for ON-SKIN EP.

20

Japan), a silicone sheet (15 × 15 ×0.8 mm; Togawa Rubber Co., Ltd., Tokushima, Japan), polyvinyl chloride tape (thickness: 0.2 mm, safety extra low voltage: ~600 V) and a silver sheet (thickness: 0.1 mm), as shown in Fig. 10a.   Positive and negative electrodes were set with 4.0-mm spacing arranged alternately, as shown in Fig. 10b. Each needle was 400 μm long with a 28° angle beveled tip, and the base diameter of the needle was approximately 200 μm, as shown in Fig. 10c.   Figure 10d shows a SEM image of one MN tip.   In order to compare the effect of IN-SKIN EP with conventional ON-SKIN EP, the needle tips of the MN array were filed and struck with a file and hammer to make them obtuse, as shown in Fig. 10e.   This obtuse tip needle array was used to apply EP at various points on the skin surface for ON-SKIN EP (where the MN electrodes were applied on skin), which was a control experiment to research the IN-SKIN EP.

The excised skin was manually punctured using the MN-electrode array with vertical pressure of 3.53 N/cm^2 for 10 sec for IN-SKIN EP, whereas for ON-SKIN EP, the pressure was set at 0.10 N/cm^2 to ensure that the needle tip did not puncture the skin.   This operation was performed on a balance to measure and control the pressure accurately.   A pulse generator (ECM 830 Electro Cell Manipulator; BTX, San Diego, CA, USA) was used to provide the square wave of EP (1 pulse/s), at 50–200 V voltage and a pulse width of 10–100 ms.

2.2.3. In vitro skin permeation experiments

The skin permeation experiment of FD-4 was performed after pretreatment of excised hairless rat skin with IN-SKIN EP, ON-SKIN EP or MN alone.   The treated skin was mounted on vertical Franz-type diffusion cells (available diffusion area: 1.77 cm^2; volume of receiver cell: 6.0 mL) immediately after the treatment, with the

stratum corneum side facing the donor compartment and the dermal side facing the receiver compartment.   The test FD-4 solution (1.0 mg/mL, 1.0 mL) was added to the donor compartment, whereas phosphate-buffered saline (PBS, pH7.4, 6.0 mL) filled the receiver compartment.   The receiver solution was stirred by a magnetic bar to ensure adequate mixing to maintain the sink condition, and was kept at 32 °C with a water jacket.

The solution was sampled at 0.5, 1.0, 2.0, 3.0, 4.0, 5.0, 6.0, 7.0 and 8.0 h after starting the permeation experiment, and the equal volume of fresh PBS was immediately added to keep the volume constant.   Intact full-thickness skin (no pretreatment) was also investigated for comparison.

FD-4 concentration in the samples was determined using a fluorospectrophotometer (RF 5300 PC; Shimadzu, Kyoto, Japan) at an excitation wavelength of 495 nm and fluorescent emission wavelength of 515 nm [64].   The calculated values for the cumulative amount of FD-4 that permeated the skin ($\mu g/cm^2$) were plotted versus time.

2.2.4. Scanning electron micrographic observation

Scanning electron microscopy (SEM, S-3000N; Hitachi High-Technologise Corp., Tokyo, Japan) was used to observe the skin surface treated by IN-SKIN EP. A skin specimen was mounted on an aluminum stub using double-sided adhesive tape and covered with gold using an ion sputter (E-1010; Hitachi High-Technologise Corp., Tokyo, Japan), with the stratum corneum facing up.   The samples were observed at 15 kV accelerating voltage and an approximately 20 mm working distance under a 30 Pa vacuum for skin samples.

2.2.5. Confocal microscopic observation of drug distribution

Confocal laser scanning was also performed for the excised hairless rat abdominal skin.   After the skin permeation experiment, the skin was taken from the diffusion cell and placed in a glass-bottomed dish (Iwaki; Asahi Glass Corp., Funabashi, Chiba, Japan), with the stratum corneum facing down, and FD-4 distribution in the skin was observed using a confocal laser scanning microscope (CLSM, Fluoview FV1000; Olympus Corp., Tokyo, Japan).   Fluorescence from the sample was excited by a 473 nm Hg laser [65].   Images were collected using FluoView software (ver. 1.5; Olympus Corp.).

2.2.6. Confocal microscopic observation (Vivascope) of puncture

The interior of the skin was observed using an *in vivo* confocal laser scanning microscope (Vivascope1500, wavelength: 830 nm; Rochester, NY, USA) to measure the actual depth of pores made by MN alone or IN-SKIN EP.   This instrument can be used to non-invasively observe the interior of tissues.   Tissue morphology up to a depth of 350 μm can be observed optically, with high sensitivity and specificity, correlating with histological sectioning [66, 67].   The punctured areas of excised abdominal skin of hairless rats were observed immediately after puncture with MN alone or IN-SKIN EP.

2.2.7. Measurement of lactate dehydrogenase (LDH) leakage from skin in vivo

Hairless rats were anesthetized by *i.p.* injection of urethane (1.0 mg/kg), and hair on the abdomen was carefully removed using an electric clipper.   A glass cell cap was attached using adhesive (Aronalpha®; Toagosei Co. Ltd., Tokyo, Japan) after pretreatment with IN-SKIN EP.   Earle's balanced salt solution (EBSS, 2.0 mL) was

then added to the glass cell cap. Whole solution was periodically collected from the glass cell cap, and the same volume of blank EBSS was added to keep the volume constant. LDH leached from the stratum corneum side was determined by an assay kit (Lactate Dehydrogenase Cytotoxicity Assay Kit; Cayman Chemical Co. Ltd., MI, U.S.A.). Non-pretreated intact skin and stripped skin were also investigated for comparison. The stripped skin was made by stripping the stratum corneum 20 times with tape. All experiments were carried out *in vivo*.

2.2.8. Statistical analysis

Statistical analysis was performed using the unpaired Student's t-test. Significant difference was accepted at 0.05. ANOVA was also applied in this study [68].

2.3. Results and discussion

2.3.1. Effect of IN-SKIN EP pretreatment on the skin permeation of FD-4

Figure 11 shows the time course of the cumulative amount of FD-4 that permeated through skin pretreated with MN, ON-SKIN EP (200 V, 10 ms, 10 pulses) or IN-SKIN EP (200 V, 10 ms, 10 pulses). The control experiment (no pretreatment) is also shown and was performed to establish a technique with reproducible results. Significant differences were found in the permeation profiles between control and pretreatment groups. Little FD-4 (0.03 $\mu g/cm^2$) was permeated through intact skin over 8 h, whereas MN and ON-SKIN EP pretreatment enhanced the FD-4 permeability approximately 7-fold (0.20 $\mu g/cm^2$) and 20-fold (0.61 $\mu g/cm^2$), respectively. Furthermore, the IN-SKIN EP showed 140-fold (4.17 $\mu g/cm^2$) permeability compared with the control permeation, suggesting a great synergistic
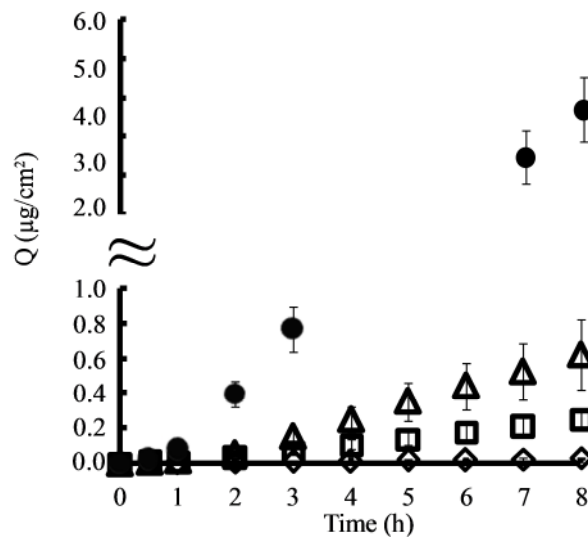
24

Fig. 11. Time course of the cumulative amount of FD-4 that permeated through intact skin, skin treated with MN alone, skin treated with ON-SKIN EP and skin treated with IN-SKIN EP. Symbols: ◇, no pretreatment (intact skin); □, MN alone; △, ON-SKIN EP (200 V, 10 ms, 10 pulses); ●, IN-SKIN EP (200 V, 10 ms, 10 pulses). Each data point represents the mean ± S.E. of four or five experiments.

effect of MN and EP on the skin permeation of FD-4.

These results, together with correlative results by conventional EP [69, 70], indicate that the IN-SKIN EP resulted in higher drug permeability with a lower voltage or shorter pulse width of EP. In addition, a higher skin penetration-enhancing effect could be obtained with IN-SKIN EP than with the previous MN-IP treatment [27], even though the permeation experiment for *in vitro* MN-IP treatment continued for 15 h.

Figure 12 shows scanning electron micrographs of intact skin (a) and skin pretreated with MN (b), ON-SKIN EP (200 V, 10 ms, 10 pulses) (c) and IN-SKIN EP (200 V, 10 ms, 10 pulses) (d). The surface of skin pretreated with IN-SKIN EP was observed to assess the effect of IN-SKIN EP to produce a transport channel across the primary barrier, the stratum corneum, against drug entry to viable tissues. The
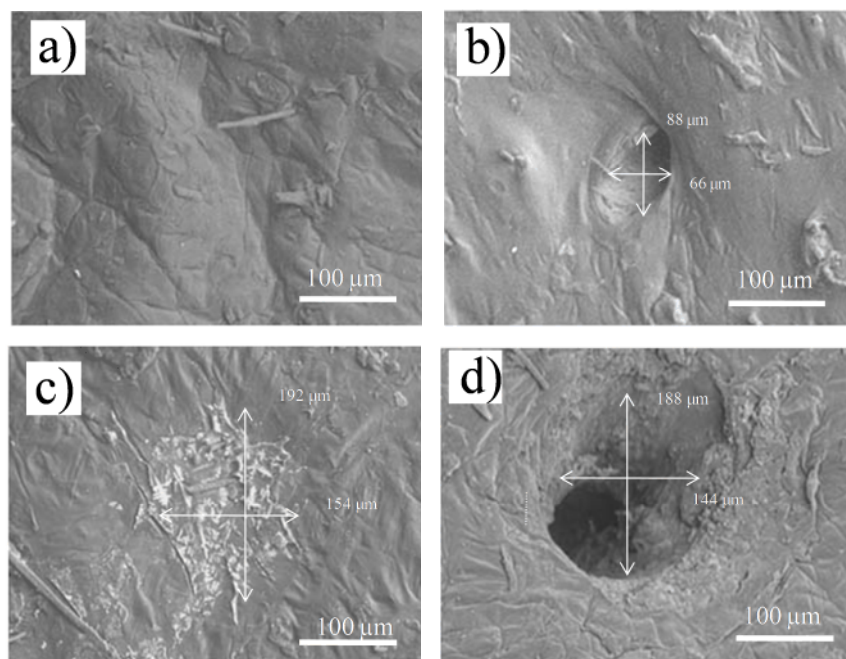
25

Fig. 12. SEM microphotograph of pores on the skin surface after pretreatment. a) Intact skin, b) MN alone, c) ON-SKIN EP (200 V, 10 ms, 10 pulses), d) IN-SKIN EP (200 V, 10 ms, 10 pulses).

diameter of the newly produced transport channels was measured horizontally and vertically, and their average size was used as an index of channel size. The average diameter of the channel produced by MN alone was 77 μm (Fig. 3b), and that by ON-SKIN EP was 168 μm (Fig. 3c), but no distinct channel was produced by ON-SKIN EP. The average diameter of the channel with IN-SKIN EP pretreatment was 166 μm (Fig. 3d). IN-SKIN EP produced the largest and deepest pore channels in skin, among the methods in the present study, and these channels would be new effective permeation pathways for chemical compounds, even macromolecules.

Intradermal distribution of FD-4 after the IN-SKIN EP pretreatment was also investigated using a CLSM. Figure 13 shows CLSM images of skin sections. It is shown from the present *in vitro* skin permeation experiments that the cumulative amount of FD-4 permeated was very limited through intact skin (Fig. 11). Correspondingly, in Fig. 13a, the average depth of fluorescent part was 20-30 μm, so

it can be considered that FD-4 was distributed only on the skin and in the stratum corneum but not permeating to the deep part of skin.   In the skin pretreated with MN (Fig. 13b), the arrow shows puncture site by MN, where the fluorescence front was about 60 μm depth.   In the ON-SKIN EP treatment (EP condition: 200 V, 10 ms, 10 pulses) (Fig. 13c), the fluorescence was distributed into deeper tissues than intact skin or MN pretreatment.   The thickness of green fluorescence in Fig. 13a-c was well correlated to the extent of skin permeation of FD-4 as shown in Fig. 11.   Although only a little difference was found among the picture in Fig. 13a-c, much deeper green trails could be clearly observed through the transport channel in skin pretreated with IN-SKIN EP (EP condition: 200 V, 10 ms, 10 pulses) (Fig. 13d).   FD-4 was
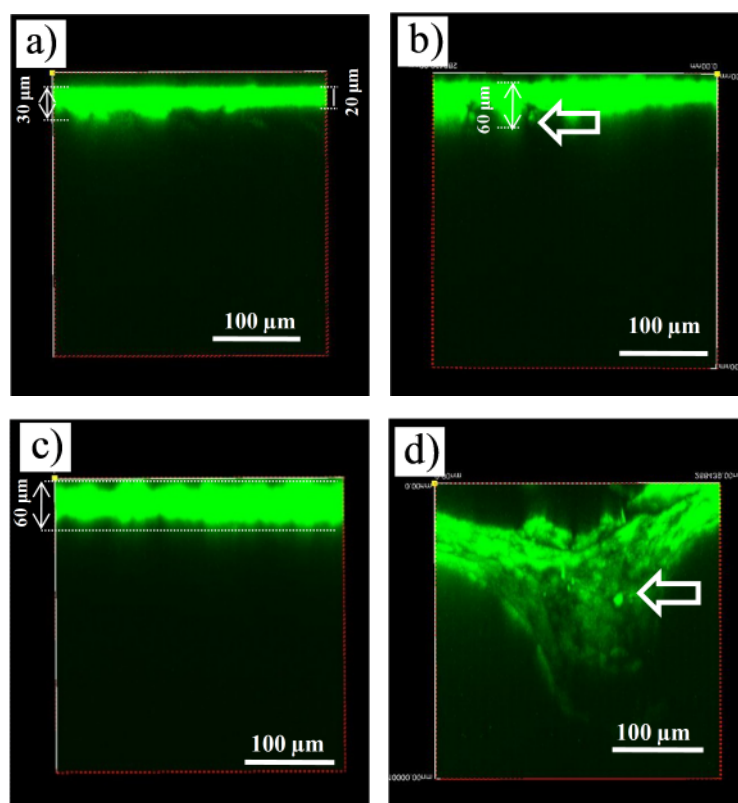

Fig. 13.   CLSM images of FD-4 distribution after 8 h permeating intact and pretreated skin.   a) Intact skin, b) MN only, c) ON-SKIN EP (200 V, 10 ms, 10 pulses), d) IN-SKIN EP (200 V, 10 ms, 10 pulses).

effectively delivered to the deep part of skin in the IN-SKIN EP.

The pore channel under the skin surface produced by MN alone and IN-SKIN EP was observed by an *in vivo* confocal laser scanning microscope. A series of pictures was taken from the surface to the deep part of the skin to analyze the depth of pores made by MN alone or IN-SKIN EP. Figure 14a–c shows skin pores (arrow) of 0.0, 10.0, and 65 μm depth, respectively, with MN alone. No pore was found in the depth of 65 μm (dotted line arrow). Although the MN electrode was 400 μm long (Fig. 10c), pore depth was less than 1/6 the full length of the MN, probably due to skin elasticity. Hairless rat skin consists of three layers: stratum corneum (approximately 0–10 μm), viable epidermis (approximately 60–90 μm) and dermis (> 90 μm) [71]. Thus, MN tips reached the viable epidermis and bypassed the stratum
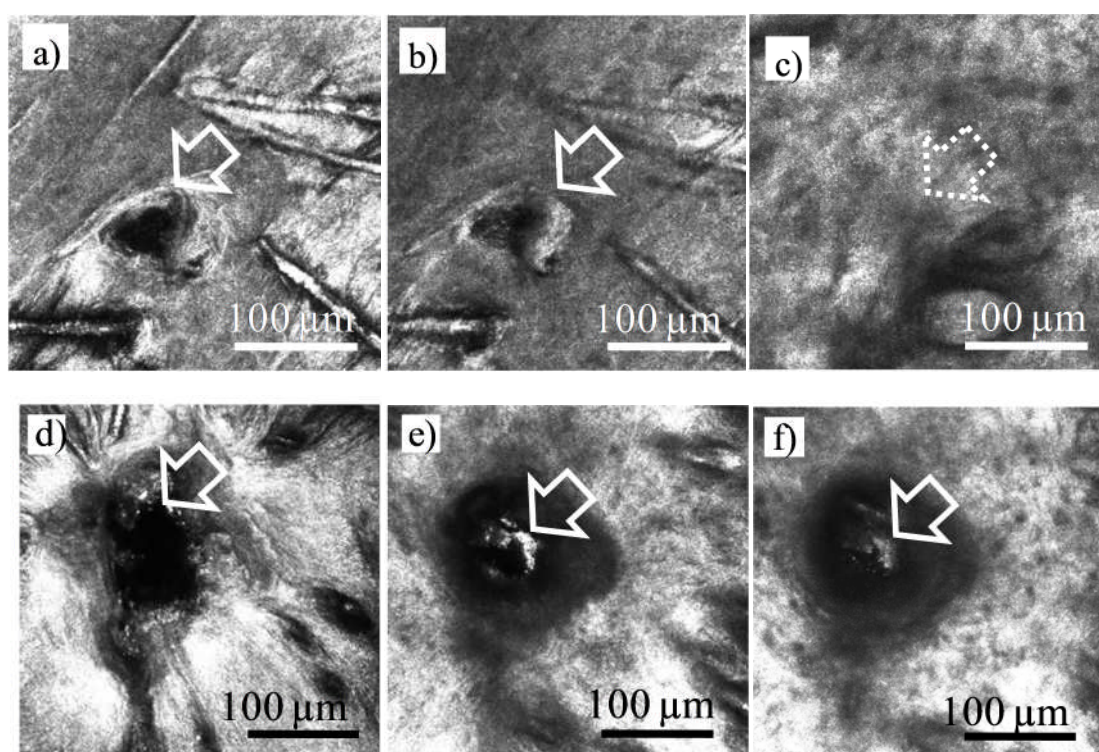

Fig. 14. *In vivo* confocal laser scanning microscopy images in the puncture direction of the pore punctured by MN alone (a–c) and IN-SKIN EP (d-f). Depth: a) 0.0 μm, b) 10.0 μm, c) 65 μm, d) 0.0 μm, e) 50 μm, f) 80 μm.

28

corneum. The holes punctured by MN therefore act as a permeation pathway for high molecular compounds.

The pores made by IN-SKIN EP were also observed. Figure 14d–f shows a similar set of images for IN-SKIN EP pretreatment to Fig. 5a–c for MN alone. EP conditions were 200 V, 10 ms and 10 pulses. Compared to Fig. 14a–c, the pores made by IN-SKIN EP were much larger and deeper. Limited by the quality of the images, data were collected until a depth of 80 μm (Fig. 14f). The pore could still be observed in the recorded depth. These data show a coincidence in depth with Fig. 13b and d. In addition, the zone of the puncture periphery, which was a circular region of approximately 100-μm diameter, was dark in the images. This could be considered a type of change in skin tissues, such as localized transport regions (LTR), as well as the Joule heat effect. Although evidence of the creation of these LTRs is still indirect in the present study, this zone is also considered as the effect of EP and acts as an important part of drug permeation [72-75].

2.3.2. Effect of voltage and pulse width in the IN-SKIN EP treatment

Figure 15 shows the effect of the application voltage and pulse width of EP on the cumulative amounts of FD-4 that permeated through skin pretreated by IN-SKIN EP (over 8 h). Voltage, pulse width and the number of pulses are the three most important parameters of the EP effect on the skin permeation [76]. In this study, the effective application period of IN-SKIN EP was fixed to 10 s, and the square wave pulse was applied at 1 pulse/s, so the number of pulses became 10. When the voltage condition was 0, 50, 100 or 150 V under a pulse width of 10 ms, the cumulative amount of FD-4 permeated through skin over 8 h was 0.20 ± 0.05, 0.23 ± 0.03, 0.64 ± 0.19 or 1.35 ± 0.91 μg/cm^2, respectively. When the pulse width was

fixed to 50 ms and the voltage condition was 50, 100 or 150 V, the cumulative

amount over 8 h was 0.33 ± 0.03, 0.81 ± 0.13 or 1.96 ± 0.64 $\mu g/cm^2$, respectively.

Based on these data, the cumulative amount over 8 h increased with the increase in

applied voltage with convex downward.   When the voltage was increased to 200 V,

the cumulative amount increased steeply.   When the voltage condition was 50 or 100

V at a pulse width of 100 ms, the cumulative amount over 8 h was 0.68 ± 0.18 or 3.00

± 0.12 $\mu g/cm^2$, respectively.   Increasing the pulse width to 100 ms is therefore an

effective way to achieve a high cumulative permeation drug amount, even at a lower

voltage.   Although either the voltage or pulse width could markedly contribute to

FD-4 permeability through excised hairless rat skin, 200 V and 10 ms pulse width

showed the highest FD-4 permeation among the conditions evaluated in this study.

No data are shown for severe IN-SKIN EP conditions, such as high voltage (> 200 V)

or long pulse width (> 100 ms), since the sink condition could not be maintained in

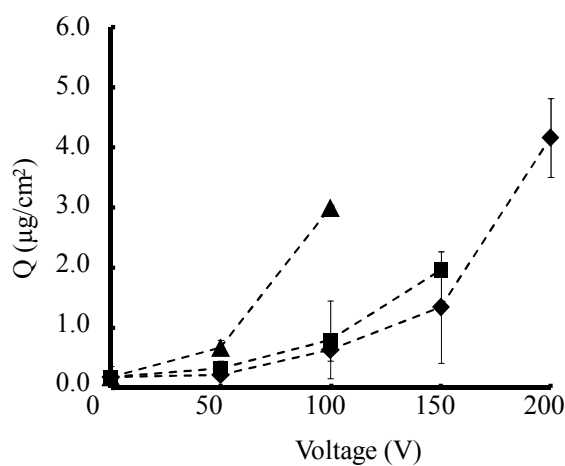the receiver solution over 8 h due to the extremely high skin permeation of FD-4.

Fig. 15.   Effect of pulse width and voltage of EP on the time course of the

cumulative amount of FD-4 that permeated hairless rat skin.   Symbols: ◆, 10 ms;

■, 50 ms; ▲, 100 ms.   Each data point represents the mean ± S.E. of four or five

experiments.

2.3.3. Influence of IN-SKIN EP on lactate dehydrogenase (LDH) leaching from skin

EP application was found to increase tissue temperature due to Joule heating [77]. It was considered from the present SEM images that a certain level of scorching was found in pores punctured by IN-SKIN EP. Cutaneous cells may be damaged when the skin is punctured by IN-SKIN EP. In order to estimate the irritation caused by IN-SKIN EP, LDH leaching from the skin was determined. The LDH leaching was used to assess skin viability [64, 78] in order to evaluate the safety of different physical enhancing methods. Two strong EP conditions (200 V, 10 ms, 10 pulses and 100 V, 100 ms, 10 pulses) were evaluated. Stripped skin was also evaluated for comparison. Figure 16 shows the cumulative amount of LDH leached from the skin surface over 1, 4 and 8 h after different pretreatments. The cumulative amount of LDH leached from stripped skin was 6.6 times that from intact skin over 8 h. In
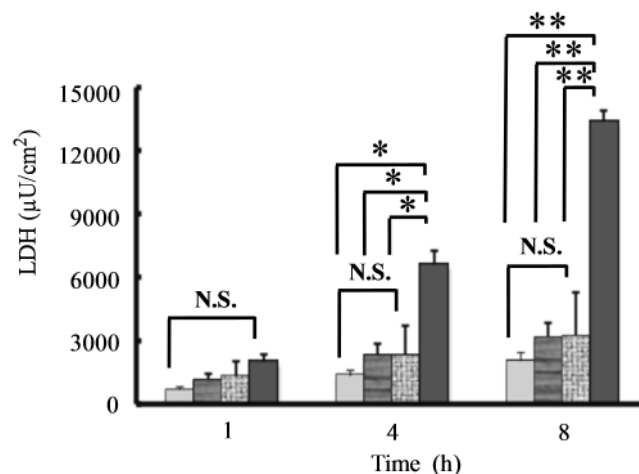
Fig. 16. Effect of different pretreatments on LDH leaching from the skin surface. Each point represents the mean ± S.E. of three or four experiments. (*: < 0.05; **: < 0.01) ☐ Intact skin, ▨ IN-SKIN EP (200 V, 10 ms, 10 pulses), ▨ IN-SKIN EP (100 V, 100 ms, 10 pulses) and ■ Stripped skin.

31

contrast, no significant difference was found between intact skin and either of the pretreatment conditions; therefore, it can be concluded that the IN-SKIN EP could create a novel permeation route to enhance the drug penetration with little damage to skin cells.

2.4. Chapter conclusion

It is important to surmount the stratum corneum barrier to increase permeability to deliver macromolecules through skin.   A novel IN-SKIN EP was developed to address this challenge in this research.   It was concluded from the present results of the *in vitro* permeation experiment of FD-4 that treatment with MN or ON-SKIN EP alone increased the permeation of FD-4 through excised hairless rat skin, and IN-SKIN EP further increased skin permeation, which was due to a great synergistic effect of MN and ON-SKIN EP.   In particular, higher permeation was achieved when applying higher voltage and longer pulse width of EP.   FD-4 was concentrated in the EP application site in this system.   In the present study, the low irritation of IN-SKIN EP could be concluded from the LDH experiment.

In conclusion, IN-SKIN EP can effectively deliver high molecular and hydrophilic drugs.   Not only drug solutions but also the topical formulations, such as gel, ointment or a patch can be applied after pretreatment with IN-SKIN EP, and could be more convenient for clinical application.

Chapter 3
Development and evaluation of the microneedle-electrode array

3.1. Introduction

The combined use of two or three physical means has been found to further increase the skin permeation of drugs [79-84]. The IN-SKIN EP, a new combination of MN and EP, was further evaluated to further increase the skin permeation of macromolecules, and the MN electrodes were arranged alternately (5 anodes and 4 cathodes) in the previous chapter. The application voltage of EP was considered to be a major determining factor for the enhancing effect [31, 85], and anode and cathode positions and the electric field strength in the stratum corneum were also shown to be important determinants for the EP effect [86, 87]. Furthermore, the electric field strength produced in the stratum corneum was closely related to the permeation amount and skin concentration of drugs [86].

Considering the distribution of the electric field on the skin, electrodes in the MN devices were set in a center-surrounding arrangement (1 cathode and 8 anodes or 1 anode and 8 cathodes). The electric field formed inside the skin barrier can be altered by changing the MN electrode position. At the same time, the effect of ON-SKIN EP was evaluated in addition to IN-SKIN EP using MN devices. The IN-SKIN EP increased the skin permeability of FD-4 more than ON-SKIN EP without severe skin damage.

In this chapter, the effects of ON-SKIN EP and IN-SKIN EP with different devices were investigated on the *in vitro* skin permeation of FD-4. In addition, changes in skin morphology were observed by a SEM after the ON-SKIN EP and IN-SKIN EP applications. The changes in skin redness and cutaneous blood flow were also investigated and used as for skin irritation.

3.2. Materials and methods

3.2.1. Chemicals and animals

The chemicals and animals used in this experiment were the same as described in Chapter 1.   The preparation of excised skin was the same as described in Chapter 2. All animal experiments were authorized by the ethics committee of Josai University (Sakado, Saitama, Japan) and conducted in according to principles of the guidelines for animal experiments at Josai University.

3.2.2. Configurations of MN-electrode array

The MN-electrode array for IN-SKIN EP was prepared by modifying the method in the previous chapter.   It was assembled using 9 acupuncture needles (Haruhari, 1.5 mm; Taiho Medical Products Co., Ltd., Hiroshima, Japan), a silicone sheet (15 × 15 ×0.8 mm; Togawa Rubber Co., Ltd., Tokushima, Japan), polyvinyl chloride tape (thickness: 0.2 mm, safety extra low voltage: ~600 V) and silver sheet (thickness: 0.1 mm).   The microneedle electrodes were arranged in the following three ways: i) anodes and cathodes were arranged alternately (device A, Fig. 17a), ii) a cathode was
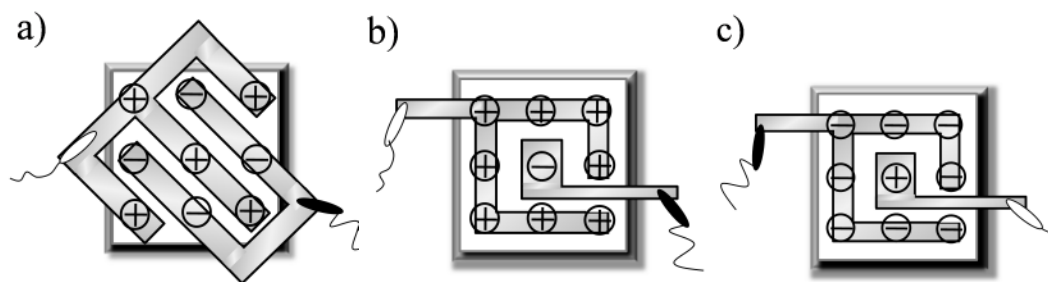

Fig. 17.   Schematic representation of three kinds of MN-electrodes array patches. MNs are arranged as a 3-by-3 array in any device.   a) 5-anodes and 4-cathodes, b) 8-anode and 1-cathode, c) 1-anode and 8- cathode.

set in the center and 8 anodes were set around the cathodes (device B, Fig. 17b) and iii) an anode was set in the center and cathodes were set around the anode (device C, Fig. 17c).   These MNs were arranged in a 3-by-3 array in all the devices, and were set with 4.0-mm spacing.   Each needle was 400 μm long with a 28° angle beveled tip, and the base diameter of the needle was approximately 200 μm.   In order to compare the effect of IN-SKIN EP with conventional ON-SKIN EP, the obtuse tip needle array was made in the same way as shown in previous chapter to apply EP at various points on the skin surface for the ON-SKIN EP.

3.2.3. Applications of IN-SKIN EP and ON-SKIN EP with MN-electrode array

The applications of IN-SKIN EP and ON-SKIN EP were the same as described in Chapter 2.

3.2.4. In vitro skin permeation experiments

The method of *in vitro* skin permeation experiment was the same as described in previous chapter.

3.2.5. Scanning electron microscopic observation

The method of scanning electron microscopic observation was the same as described in previous chapter.

3.2.6. Measurement of skin redness and cutaneous blood flow

The skin redness and cutaneous blood flow were determined on a scale of the indeces of skin irritation [88].   The study was performed at ambient temperature (24 ± 1 °C).   Three circular areas with a diameter of 1 cm were marked on the abdomen

of each hairless rat.   The skin color was measured using a Minolta CR-400 chromameter (Konicaminolta Sensing Inc., Osaka, Japan). The chromameter was rectified before measuring the skin using the color standard (Perimed AB, Jarfalla, Sweden).   The detection head of the chromameter was placed gently onto the skin to measure the skin color, and the value of a^* (AU) was recorded.   Subcutaneous blood flow was imaged before application of the MN-electrode arrays with a laser Doppler perfusion imager (LDPI; Perimed AB) and PeriScan PIM 3 (Perimed AB) to avoid the vein, which would interfere with blood flow measurements before application of the MN-electrode arrays.   The distance between the LDPI measuring head and the skin surface was set at 20 cm and the images were analyzed by calculating the mean blood flow over the marked area within the abdomen skin, corresponding to the size of the mold of the MN array.   Blood flow was expressed as perfusion units (PU).   Skin redness and cutaneous blood flow were determined after the following treatments: (i) non-pretreated skin as a negative control, (ii) MN alone, (iii) IN-SKIN EP (50 V, 100 ms, 10 pulses), (iv) ON-SKIN EP (50 V, 100 ms, 10 pulses) and (v) IN-SKIN EP (100 V, 100 ms, 10 pulses).

The skin redness and cutaneous blood flow were measured 0, 15, 30, 45, 60, 90 and 120 min after application.   Before applying the MN arrays or IN-SKIN EP, baseline values were recorded for the cutaneous blood flow and skin color.

3.2.7 In vivo experiment

The hairless rats were anesthetized by peritoneal injection of urethane (1.0 g/kg) and the hair on the abdomen was carefully shaved using an electric clipper.   Their body temperature was maintained at 36.5 ± 0.5 °C throughout the experiments with a piece of electric carpet.   An area of skin on the abdomen was manually punctured

using the MN-electrode array with vertical pressure of 3.53 N/cm^2 for 10 sec in the IN-SKIN EP application with the device B.   Then, a donor cell was immobilized onto the punctured area by adhesive compound.   The test FD-4 solution (1.0 mg/mL, 1.0 mL) was added to the donor cell.   The preparation of blood samples was the same as in *1.2.5.*, and plasma samples were measured by using the method in *1.2.8.*

3.2.8. Statistical analysis

Statistical analysis was performed using Student's t-test and ANOVA.   A *p* value less than 0.05 was considered significant.

3.3. Results and discussion

3.3.1. Effect of IN-SKIN EP pretreatment on the skin permeation of FD-4

Figure 18a and b show the time courses of the cumulative amount of FD-4 that permeated skin pretreated with ON-SKIN EP (50 V, 100 ms, 10 pulses) and IN-SKIN
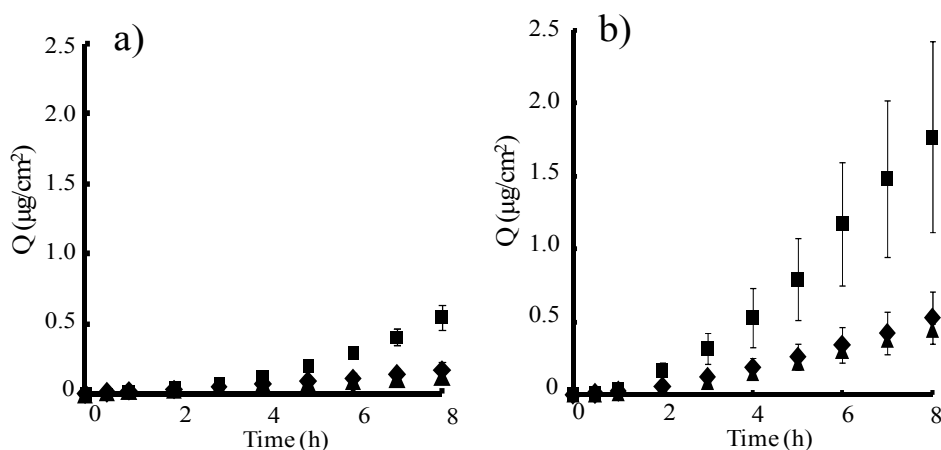

Fig. 18.   Time courses of the cumulative amount of FD-4 that permeated through skin pretreated by ON-SKIN EP (a) and IN-SKIN EP (b) with three kinds of devices. Symbols: ◆, device A; ■device B; ▲, device C. (EP condition: 50 V, 100 ms, 10 pulses)

37

EP (50 V, 100 ms, 10 pulses), respectively.   While the cumulative amount of FD-4 permeated through the skin was 0.03 ± 0.002 µg/cm^2 over 8h for the non-pretreatment group [89], the corresponding values for the ON-SKIN EP using devices A, B and C were approximately 6-fold (0.17 ± 0.06 µg/cm^2), 18-fold (0.54 ± 0.09 µg/cm^2) and 4-fold (0.13 ± 0.02 µg/cm^2) higher, respectively, than the non-pretreatment group. Device B showed the highest permeation-enhancing effect.

On the other hand, the permeation-enhancing effect over 8 h by IN-SKIN EP using device A, B and C was nearly18-fold (0.53 ± 0.18 µg/cm^2), 59-fold (1.77 ± 0.65 µg/cm^2) and 15-fold (0.44 ± 0.04 µg/cm^2), respectively, in comparison with the non-pretreatment group.   Device B also showed the highest effect by the IN-SKIN EP.   The order of the penetration-enhancing effect was device B >> device A > device C both for the ON-SKIN EP and IN-SKIN EP applications.   In addition, it is clear that the IN-SKIN EP had a much higher penetration-enhancing effect than the
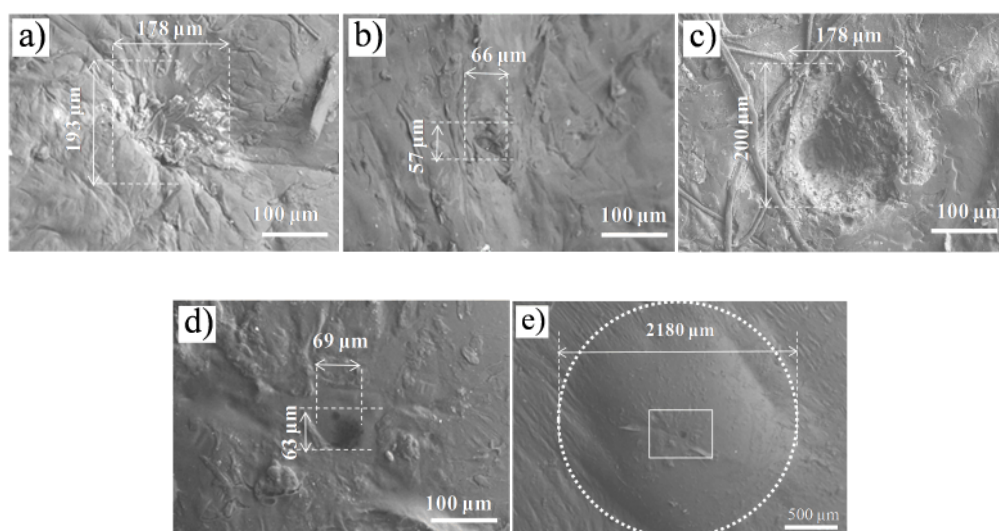

Fig. 19.   SEM microphotograph of the skin surface after application of IN-SKIN EP and ON-SKIN EP with different electrode (EP condition: 50 V, 100 ms, 10 pulses). (a) ON-SKIN EP (anode), (b) ON-SKIN EP (cathode), (c) IN-SKIN EP (anode), (d) IN-SKIN EP (cathode), and (e) Enlarged drawing of Fig. 3d, the ring shows edematous swelling around the pore.

ON-SKIN EP when applying the same voltage with the same pulse width.

3.3.2. Scanning electron micrographic observation

Figure 19 shows SEM photographs of the effect of ON-SKIN EP and IN-SKIN EP by a single needle on the skin surface. All of the EP treatments were performed using a single pair of electrodes under conditions of 50 V, 100 ms and 10 pulses, which were the same conditions as in the skin permeation experiment. The ON-SKIN EP showed moderate change of the skin surface morphology (Fig. 19a and b). On the other hand, the IN-SKIN EP produces transport channels across the primary barrier, the stratum corneum, for macromolecular drug entry into viable tissues (Fig. 19c and d). The pore channels produced by the IN-SKIN EP which functioned as new and effective pathways of chemical compounds through skin, and such channels could be utilized for the skin permeation pathway for high molecular compounds as well as low molecular compounds. The diameter of the produced transport channels in the skin was measured, and their average size was used as an index of the channel size. The average diameter of the marks produced by the anodes and cathodes for the ON-SKIN EP was calculated to be 186 μm (Fig. 19a) and 62 μm (Fig. 19b), respectively. In the case of IN-SKIN EP, the average diameter of the channel produced by the anode was 199 μm (Fig. 19c), with 66 μm for the cathode (Fig. 19d). The size of pores created by a single pair of electrodes corresponded to that by MN-electrodes array devices (device A, B and C) (data not shown). According to these SEM observations, the anodes were found to contribute more to the drug delivery pathway than the cathodes. These data above were closely related to device B showing the highest permeation-enhancing effect, and device C showing the lowest effect among three devices (Fig. 18).

Interestingly, edema was found around the pore, with a diameter of about 1 mm, as shown in Fig. 19e under a lower multiplying factor, in skin pretreated by the cathode. On the other hand, no such edema could be found in the skin after pretreatment by the anode. Water flux (electrosmosis) from the anode to cathode may be the reason for the edema under the cathode.

3.3.3. Influence of IN-SKIN EP on skin redness and blood flow

Because heat-generated wave of EP propagates outward from the applied site [90], EP pretreatment might affect the deeper tissues under the skin surface, even cutaneous capillary vessels. Hence, the changes in skin redness and blood flow were further evaluated in the present study. The irritation index was measured both with a chromameter and an LDPI. Both apparatuses can measure the erythema in skin. The chromameter evaluates skin surface redness, while the LDPI measures blood flow in much deeper skin layers. The exact penetration depth of the laser depends on the extent of pigmentation, but the obtained image reflects cutaneous blood flow with a depth less than 1 mm [91]. The redness and blood flow after IN-SKIN EP treatment were evaluated under the same conditions as in the skin permeation experiment (50 V, 100 ms, 10 pulses). MN treatment and ON-SKIN EP treatment (50 V, 100 ms, 10 pulses) were also evaluated for comparison.

Safety evaluation was conducted using device B and device C, which showed the highest and lowest skin permeation-enhancing effects, respectively. Figure 20 shows the change in redness (Δa) for devices B and C. The shadow part in Fig. 20 represents the variation in redness for non-pretreatment (control). In the present study, the variation of control was determined as an acceptable range for all pretreatments. Skin redness did not change markedly: IN-SKIN EP treatment

resulted in the maximum Δa values 15 min after application, 0.36 ± 0.09 absorption units (AU) for device B and 0.22 ± 0.14 AU for device C; however, these maximum values returned to the control value within 45 min. MN and ON-SKIN EP did not show more irritation than the non-treatment group.

The change in blood flow showed a similar tendency to that in skin redness
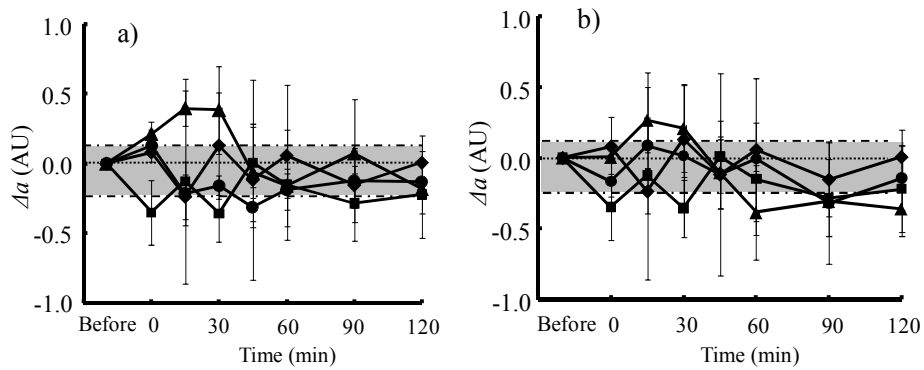

Fig. 20. The change in skin redness at different time points after pretreatment of device B (a) and device C (b).

Symbols: ◆, non-pretreatment, ■, MN alone; ●, ON-SKIN EP (50 V, 100 ms, 10 pulses); ▲, IN-SKIN EP (50 V, 100 ms, 10 pulses).
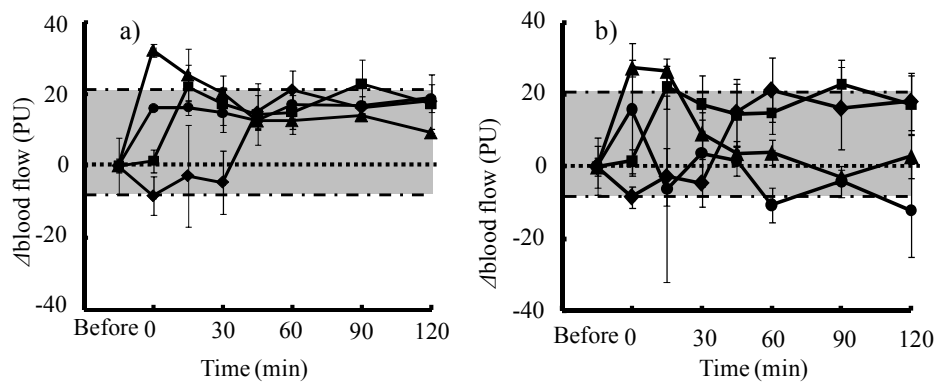

Fig. 21. The change in blood flow at different time points after pretreatment of device B (a) and device C (b).

Symbols: ◆, non-pretreatment, ■, MN alone; ●, ON-SKIN EP (50 V, 100 ms, 10 pulses); ▲, IN-SKIN EP (50 V, 100 ms, 10 pulses).

(Fig. 21).   The maximal blood flow was observed immediately after IN-SKIN EP treatment.   The vasodilation response caused by the inflammatory reaction in the dermis must be faster than the redness response on the skin surface.   The maximum values were 29 ± 3 PU and 26 ± 6 PU for device B and C, respectively, and returned to the acceptable range within 15 min.

No significant difference was observed in skin redness and cutaneous blood flow between devices B and C ($P < 0.01$).   These data suggest that the EP condition (50 V, 100 ms, 10 pulses) in the present *in vitro* study could be considered safe.

Next, the effect of EP voltage on redness and blood flow was investigated.   As shown in Fig. 22a and b, EP treatment with 100 V resulted in significantly higher redness (1.61 ± 0.41 AU) and greater blood flow (97 ± 5 PU), respectively, than non-pretreatment skin, for device B after application ($P < 0.01$).

The blood flow returned to the acceptable range within 45 min and redness remained until 90 min, which indicated a longer irritation period than EP treatment with 50 V.
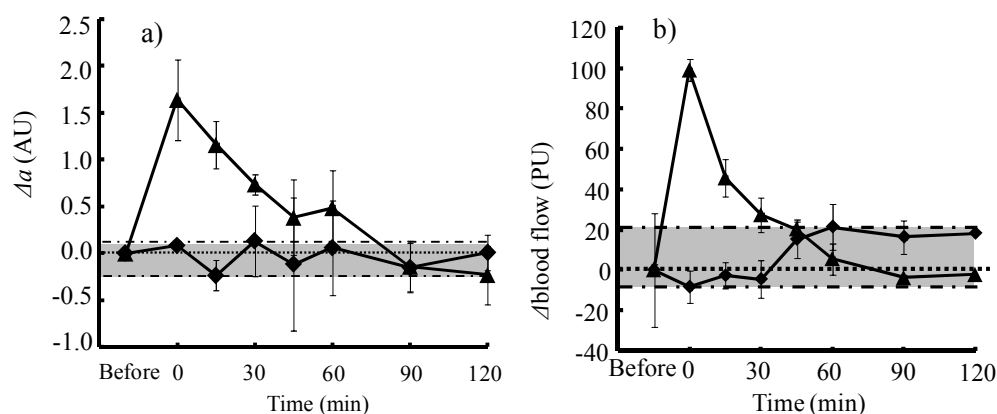

Fig. 22.   The change in redness (a) and blood flow (b) at different time points after pretreatment of IN-SKIN EP (100 V, 100 ms, 10 pulses) with device B.   Symbols: ◆, non-pretreatment;   ▲, IN-SKIN EP (100 V, 100 ms, 10 pulses).
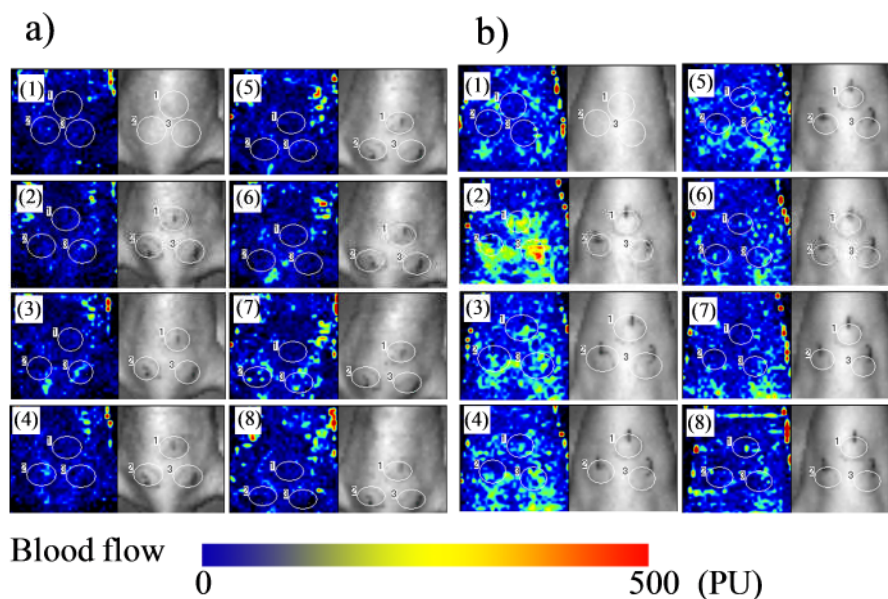
Fig. 23. Laser doppler perfusion images and pictures of hairless rat abdomen skin. The images show the change in blood flow at different time points. (a) skin without pretreatment, (b) the skin after the pretreatment of IN-SKIN EP (100 V, 100 ms, 10 pulses). The time points: (1) before, (2) 0 min (just after application), (3) 15 min, (4) 30 min, (5) 45 min, (6) 60 min, (7) 90 min and (8) 120 min.

Subcutaneous blood flow was also monitored by an LDPI. Figure 23b shows representative pictures and perfusion images of skin after IN-SKIN EP application (100 V, 100 ms, 10 pulses) with device B. These images show the same skin area before and after treatment at different time points. Figure 23a shows those for non-pretreatment. The applied area in the perfusion image turned red and then returned to normal within 45 min after IN-SKIN EP application (Fig. 23b) compared to non-pretreatment (Fig. 23a). These results might indicate that the increase of voltage increases the skin irritation by the IN-SKIN EP.

In vivo experiment was performed to evaluate the effect of the IN-SKIN EP means on the skin permeation of drugs. Plasma concentration-time profiles of FD-4 after *i.c.* injection with a 33 G needle and IN-SKIN EP pretreatment were
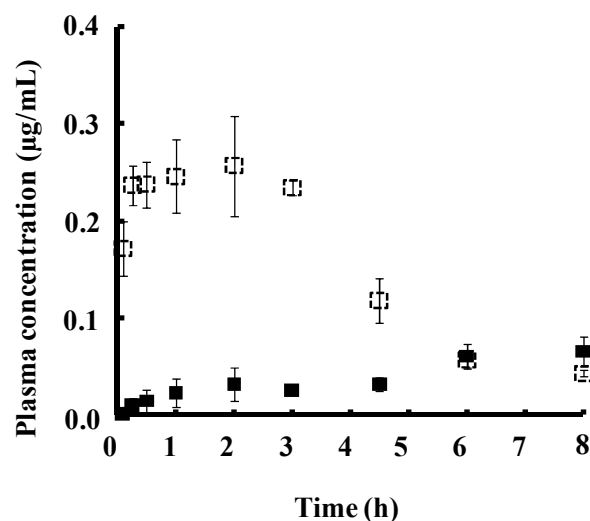
43

Fig. 24.　Time course of plasma concentration of FD-4 after *i.c.* injection with 33 G-needle and IN-SKIN EP application in the abdomen of rats.　*I.c.* injection data are the same as in Fig. 3.　Symbols: □ *i.c.*, ■ IN-SKIN EP.

compared in Fig. 24.　The *i.c.* injection showed a higher C_{max} (0.25 ± 0.04 μg/mL) at 120 min; but it showed a lower plasma level (0.04 ± 0.01 μg/mL) at the last stage (8 h).　On the other hand, the IN-SKIN EP pretreatment showed continuous plasma level despite of lower absorption rate.　IN-SKIN EP also displayed a higher plasma level 8 h after starting the experiment (0.69 ± 0.02 μg/mL), thus, much more FD-4 can be absorbed into the systemic circulation after 8 h.

3.4. Chapter conclusion

IN-SKIN EP proved to be a more promising means than ON-SKIN EP to increase the skin permeability of macromolecules.　Three kinds of microneedle-electrode array device for the IN-SKIN EP application were evaluated.　The IN-SKIN EP increased the skin permeation of FD-4.　Device B with one central cathode and 8 surrounding anodes showed the most significant permeation-enhancing effect.　In addition, the IN-SKIN EP did not show any severe skin irritation.

44

Conclusion

The following conclusion can be obtained from the present results:

(1) 33 G-needles could provide less invasive injection and more steady plasma drug level. *I.c.* injection showed a higher absorption than *s.c.* and *i.m.* injection for a model macromolecule, FD-4, so the feasibility of the transdermal delivery of macromolecules was expected.

(2) IN-SKIN EP can effectively deliver high molecular and hydrophilic drugs, which was probably due to a great synergistic effect by MN and ON-SKIN EP. In particular, higher permeation of FD-4 was achieved when applying higher voltage and longer pulse width of EP.

(3) The anode and cathode positions and the electric field strength in the stratum corneum were the important determinants for the EP effect. The device with one central cathode and 8 surrounding anodes showed the most significant permeation-enhancing effect of FD-4 through skin. Besides, the IN-SKIN EP did not show any severe irritation on skin.

The presently proposed IN-SKIN EP is able to overcome the stratum corneum barrier with only minimal irritation, which opens the opportunity for dermal and transdermal delivery of high molecular weight/high hydrophilic drugs together for vaccine delivery.

References

[1] C.S. Asbill, B.B. Michniak, Percutaneous penetration enhancers: local versus transdermal activity. *Pharm. Sci. Technol. Today* **3**(1) (2000) 36-41.

[2] J.P. Jonathan Hadgraft, Dafydd G. Williams, W. John Pugh, Geoffrey Allan, Mechanisms of action of skin penetration enhancers/retarders: Azone and analogues. *Int. J. Pharm.* **141**(1-2) (1996) 17-25.

[3] M. Kirjavainen, J. Monkkonen, M. Saukkosaari, R. Valjakka-Koskela, J. Kiesvaara, A. Urtti, Phospholipids affect stratum corneum lipid bilayer fluidity and drug partitioning into the bilayers. *J. Control. Release* **58**(2) (1999) 207-214.

[4] S. Parsaee, M.N. Sarbolouki, M. Parnianpour, In-vitro release of diclofenac diethylammonium from lipid-based formulations. *Int. J. Pharm.* **241**(1) (2002) 185-190.

[5] H.O. Ho, F.C. Huang, T.D. Sokoloski, M.T. Sheu, The influence of cosolvents on the in-vitro percutaneous penetration of diclofenac sodium from a gel system. *J. Pharm. Pharmacol.* **46**(8) (1994) 636-642.

[6] S.C. Shin, H.J. Kim, I.J. Oh, C.W. Cho, K.H. Yang, Development of tretinoin gels for enhanced transdermal delivery. *Eur. J. Pharm. Biopharm.* **60**(1) (2005) 67-71.

[7] D.J. Crommelin, G. Storm, R. Verrijk, L. de Leede, W. Jiskoot, W.E. Hennink, Shifting paradigms: biopharmaceuticals versus low molecular weight drugs. *Int. J. Pharm.* **266**(1-2) (2003) 3-16.

[8] J.D. Bos, M.M. Meinardi, The 500 Dalton rule for the skin penetration of chemical compounds and drugs. *Exp. Dermatol.* **9**(3) (2000) 165-169.

[9] J.H. Oh, H.H. Park, K.Y. Do, M. Han, D.H. Hyun, C.G. Kim, C.H. Kim, S.S. Lee, S.J. Hwang, S.C. Shin, C.W. Cho, Influence of the delivery systems using a microneedle array on the permeation of a hydrophilic molecule, calcein. *Eur. J. Pharm. Biopharm.* **69**(3) (2008) 1040-1045.

[10] Y.W. Chien, A.K. Banga, Iontophoretic (transdermal) delivery of drugs: overview of historical development. *J. Pharm. Sci.* **78**(5) (1989) 353-354.

[11] M.R. Prausnitz, V.G. Bose, R. Langer, J.C. Weaver, Electroporation of mammalian skin: a mechanism to enhance transdermal drug delivery. *Proc. Natl. Acad. Sci. U. S. A.* **90**(22) (1993) 10504-10508.

[12] S. Mitragotri, D. Blankschtein, R. Langer, Ultrasound-mediated transdermal protein delivery. *Science* **269**(5225) (1995) 850-853.

[13] D.V. McAllister, P.M. Wang, S.P. Davis, J.H. Park, P.J. Canatella, M.G. Allen, M.R. Prausnitz, Microfabricated needles for transdermal delivery of macromolecules and nanoparticles: fabrication methods and transport studies. *Proc. Natl. Acad. Sci. U. S. A.* **100**(24) (2003) 13755-13760.

[14] K.S. Bhatia, J. Singh, Effect of linolenic acid/ethanol or limonene/ethanol and iontophoresis on the in vitro percutaneous absorption of LHRH and ultrastructure of human epidermis. *Int. J. Pharm.* **180**(2) (1999) 235-250.

[15] S. Kaushik, A.H. Hord, D.D. Denson, D.V. McAllister, S. Smitra, M.G. Allen, M.R. Prausnitz, Lack of pain associated with microfabricated microneedles. *Anesth. Analg.* **92**(2) (2001) 502-504.

[16] D.V. McAllister, P.M. Wang, S.P. Davis, J.H. Park, P.J. Canatella, M.G. Allen, M.R. Prausnitz, Microfabricated needles for transdermal delivery of macromolecules and nanoparticles: fabrication methods and transport studies. *Proc. Natl. Acad. Sci. U. S. A.* **100**(24) (2003) 13755-13760.

[17] S. Kaushik, A.H. Hord, D.D. Denson, D.V. McAllister, S. Smitra, M.G. Allen, M.R. Prausnitz, Lack of pain associated with microfabricated microneedles. *Anesth. Analg.* **92**(2) (2001) 502-504.

[18] X.M. Wu, H. Todo, K. Sugibayashi, Enhancement of skin permeation of high

molecular compounds by a combination of microneedle pretreatment and iontophoresis. *J. Control. Release* **118**(2) (2007) 189-195.

[19] W. Martanto, S.P. Davis, N.R. Holiday, J. Wang, H.S. Gill, M.R. Prausnitz, Transdermal delivery of insulin using microneedles in vivo. *Pharm. Res.* **21**(6) (2004) 947-952.

[20] W. Lin, M. Cormier, A. Samiee, A. Griffin, B. Johnson, C.L. Teng, G.E. Hardee, P.E. Daddona, Transdermal delivery of antisense oligonucleotides with microprojection patch (Macroflux) technology. *Pharm. Res.* **18**(12) (2001) 1789-1793.

[21] J.A. Matriano, M. Cormier, J. Johnson, W.A. Young, M. Buttery, K. Nyam, P.E. Daddona, Macroflux microprojection array patch technology: a new and efficient approach for intracutaneous immunization. *Pharm. Res.* **19**(1) (2002) 63-70.

[22] U.O. Hafeli, A. Mokhtari, D. Liepmann, B. Stoeber, In vivo evaluation of a microneedle-based miniature syringe for intradermal drug delivery. *Biomed. Microdevices* **11** (2009) 943–950.

[23] G. Li, A. Badkar, S. Nema, C.S. Kolli, A.K. Banga, In vitro transdermal delivery of therapeutic antibodies using maltose microneedles. *Int. J. Pharm.* **368**(1-2) (2009) 109-115.

[24] Z. Ding, F.J. Verbaan, M. Bivas-Benita, L. Bungener, A. Huckriede, D.J. van den Berg, G. Kersten, J.A. Bouwstra, Microneedle arrays for the transcutaneous immunization of diphtheria and influenza in BALB/c mice. *J. Control. Release* **136**(1) (2009) 71-78.

[25] B. Al-Qallaf, D.B. Das, Optimizing microneedle arrays to increase skin permeability for transdermal drug delivery. *Ann. N. Y. Acad. Sci.* **1161**(2009) 83-94.

[26] M.M. Badran, J. Kuntsche, A. Fahr, Skin penetration enhancement by a

microneedle device (Dermaroller) in vitro: dependency on needle size and applied formulation. *Eur. J. Pharm. Sci.* **36**(4-5) (2009) 511-523.

[27] X.M. Wu, H. Todo, K. Sugibayashi, Enhancement of skin permeation of high molecular compounds by a combination of microneedle pretreatment and iontophoresis. *J. Control. Release* **118**(2) (2007) 189-195.

[28] U. Zimmermann, J. Schulz, G. Pilwat, Transcellular ion flow in Escherichia coli B and electrical sizing of bacterias. *Biophys. J.* **13**(10) (1973) 1005-1013.

[29] E. Neumann, K. Rosenheck, Permeability changes induced by electric impulses in vesicular membranes. *J. Membr. Biol.* **10**(3) (1972) 279-290.

[30] M.R. Prausnitz, E.R. Edelman, J.A. Gimm, R. Langer, J.C. Weaver, Transdermal delivery of heparin by skin electroporation. *Biotechnology* **13**(11) (1995) 1205-1209.

[31] T. Chen, R. Langer, J.C. Weaver, Charged microbeads are not transported across the human stratum corneum in vitro by short high-voltage pulses. *Bioelectrochem. Bioenerg.* **48**(1) (1999) 181-192.

[32] B.M. Medi, J. Singh, Electronically facilitated transdermal delivery of human parathyroid hormone (1-34). *Int. J. Pharm.* **263**(1-2) (2003) 25-33.

[33] T.W. Wong, C.H. Chen, C.C. Huang, C.D. Lin, S.W. Hui, Painless electroporation with a new needle-free microelectrode array to enhance transdermal drug delivery. *J. Control. Release* **110**(3) (2006) 557-565.

[34] S. Tokumoto, N. Higo, K. Sugibayashi, Effect of electroporation and pH on the iontophoretic transdermal delivery of human insulin. *Int. J. Pharm.* **326**(1-2) (2006) 13-19.

[35] Q. Xu, R.P. Kochambilli, Y. Song, J. Hao, W.I. Higuchi, S.K. Li, Effects of alternating current frequency and permeation enhancers upon human epidermal membrane. *Int. J. Pharm.* **372**(1-2) (2009) 24-32.

[36] F. Marra, J.L. Levy, P. Santi, Y.N. Kalia, In vitro evaluation of the effect of electrotreatment on skin permeability. *J. Cosmet. Dermatol.* **7**(2) (2008) 105-111.

[37] J.Y. Fang, C.F. Hung, T.L. Hwang, W.W. Wong, Transdermal delivery of tea catechins by electrically assisted methods. *Pharmacol. Physiol.* **19**(1) (2006) 28-37.

[38] T.R. Gowrishankar, T.O. Herndon, J.C. Weaver, Transdermal drug delivery by localized intervention. *Eng. Med. Biol. Mag.* **28**(1) (2009) 55-63.

[39] S.M. Sammeta, S.R. Vaka, S. Narasimha Murthy, Transdermal drug delivery enhanced by low voltage electropulsation (LVE). *Pharm. Dev. Technol.* **14**(2) (2009) 159-164.

[40] C.P. Zhou, Y.L. Liu, H.L. Wang, P.X. Zhang, J.L. Zhang, Transdermal delivery of insulin using microneedle rollers in vivo. *Int. J. Pharm.* **392**(2010) 127-133.

[41] Y. Tokudome, K. Sugibayashi, Mechanism of the synergic effects of calcium chloride and electroporation on the in vitro enhanced skin permeation of drugs. *J. Control. Release* **95**(2) (2004) 267-274.

[42] A. Mailis-Gagnon, G.J. Bennett, Abnormal contralateral pain responses from an intradermal injection of phenylephrine in a subset of patients with complex regional pain syndrome (CRPS). *Pain* **111**(3) (2004) 378-384.

[43] I. Leroux-Roels, E. Vets, R. Freese, M. Seiberling, F. Weber, C. Salamand, G. Leroux-Roels, Seasonal influenza vaccine delivered by intradermal microinjection: A randomised controlled safety and immunogenicity trial in adults. *Vaccine* **26**(51) (2008) 6614-6619.

[44] P.H. Lambert, P.E. Laurent, Intradermal vaccine delivery: will new delivery systems transform vaccine administration? *Vaccine* **26**(26) (2008) 3197-3208.

[45] R. Han, C.A. Reed, N.M. Cladel, N.D. Christensen, Immunization of rabbits with cottontail rabbit papillomavirus E1 and E2 genes: protective immunity induced by

gene gun-mediated intracutaneous delivery but not by intramuscular injection. *Vaccine* **18**(26) (2000) 2937-2944.

[46] Y. Xia, E. Chen, D.L. Tibbits, T.E. Reilley, T.D. McSweeney, Comparison of effects of lidocaine hydrochloride, buffered lidocaine, diphenhydramine, and normal saline after intradermal injection. *J. Clin. Anesth.* **14**(5) (2002) 339-343.

[47] E.K. Zsigmond, P. Darby, H.M. Koenig, E.F. Goll, Painless intravenous catheterization by intradermal jet injection of lidocaine: a randomized trial. *J. Clin. Anesth.* **11**(2) (1999) 87-94.

[48] R.H. Guy, Current status and future prospects of transdermal drug delivery. *Pharm. Res.* **13**(12) (1996) 1765-1769.

[49] M.R. Prausnitz, Reversible skin permeabilization for transdermal delivery of macromolecules. Crit. Rev. Ther. *Drug Carrier Syst.* **14**(4) (1997) 455-483.

[50] D. Yoshida, T. Hasegawa, K. Sugibayashi, Targeting of salicylate to skin and muscle following topical injections in rats. *Int. J. Pharm.* **231**(2) (2002) 177-184.

[51] D. Yoshida, H. Todo, T. Hasegawa, K. Sugibayashi, Dermatopharmacokinetics of salicylate following topical injection in rats: effect of osmotic pressure and injection volume on salicylate disposition. *Int. J. Pharm.* **337**(1-2) (2007) 142-147.

[52] D. Yoshida, H. Todo, T. Hasegawa, K. Sugibayashi, Effect of molecular weight on the dermatopharmacokinetics and systemic disposition of drugs after intracutaneous injection. *Eur. J. Pharm. Sci.* **35**(1-2) (2008) 5-11.

[53] D. Yoshida, H. Todo, T. Hasegawa, K. Sugibayashi, Effect of vasoactive agents on the dermatopharmacokinetics and systemic disposition of model compounds, salicylate and FITC-dextran 4 kDa, following intracutaneous injection of the compounds. *Int. J. Pharm.* **356**(1-2) (2008) 181-186.

[54] R.J. Scheuplein, Mechanism of percutaneous absorption. II. Transient diffusion

and the relative importance of various routes of skin penetration. *J. Invest. Dermatol.* **48**(1) (1967) 79-88.

[55] R.J. Scheuplein, I.H. Blank, Mechanism of percutaneous absorption. IV. Penetration of nonelectrolytes (alcohols) from aqueous solutions and from pure liquids. *J. Invest. Dermatol.* **60**(5) (1973) 286-296.

[56] M. Morishita, N. Kamei, J. Ehara, K. Isowa, K. Takayama, A novel approach using functional peptides for efficient intestinal absorption of insulin. *J. Control. Release* **118**(2) (2007) 177-184.

[57] R.R. Levine, W.F. McNary, P.J. Kornguth, R. LeBlanc, Histological reevaluation of everted gut technique for studying intestinal absorption. *Eur. J. Pharm.* **9**(2) (1970) 211-219.

[58] J.L. Richardson, P.S. Minhas, N.W. Thomas, L. Illum, Vaginal administration of propranolol to rats: Absorption and histological effects on the vaginal epithelium. *Int. J. Pharm.* **56**(1989) R1-R4.

[59] S.G. Chandler, L. Illum, N.W. Thomas, Nasal absorption next in the rat. I: A method to demonstrate the histological effects of nasal formulations. *Int. J. Pharm.* **70** (1991) 19-27.

[60] P.U. Jani, A.T. Florence, D.E. McCarthy, Further histological evidence of the gastrointestinal absorption of polystyrene nanospheres in the rat. *Int. J. Pharm.* **84** (1992) 245-252.

[61] FDA, Guidance for Industry: Bioavailability and Bioequivalence Studies for Orally Administered Drug Products — General Considerations.   (2003).

[62] D.X. Cao, Yuko Tazawa, H. Ishii, H. Todo, K. Sugibayashi., Pretreatment effects of moxibustion on the skin permeation and skin and muscle concentrations of salicylate in rats. *Int. J. Pharm*. **407**(2011) 105-110.

[63] M. Rücker, F. Roesken, B. Vollmar, M.D. Menger, A novel approach for comparative study of periosteum, muscle, subcutis, and skin microcirculation by intravital fluorescence microscopy. *Microvasc. Res.* **56**(1) (1998) 30-42.

[64] X.M. Wu, H. Todo, K. Sugibayashi, Effects of pretreatment of needle puncture and sandpaper abrasion on the in vitro skin permeation of fluorescein isothiocyanate (FITC)-dextran. *Int. J. Pharm.* **316**(1-2) (2006) 102-108.

[65] M.S. Rujirat Santipanichwong, Influence of different *β*-glucans on the physical and rheological properties of egg yolk stabilized oil-in-water emulsions. *Food Hydrocolloids* **23**(5) (2009) 1279-1287

[66] M.A. Altintas, A.A. Altintas, M. Guggenheim, K. Knobloch, A.D. Niederbichler, P.M. Vogt, Monitoring of microcirculation in free transferred musculocutaneous latissimus dorsi flaps by confocal laser scanning microscopy - a promising non-invasive methodical approach. *J. Plast. Reconstr. Aesthet. Surg.* **63**(1) (2008) 111-117.

[67] M.A. Altintas, A.A. Altintas, K. Knobloch, M. Guggenheim, C.J. Zweifel, P.M. Vogt, Differentiation of superficial-partial vs. deep-partial thickness burn injuries in vivo by confocal-laser-scanning microscopy. *Burns* **35**(1) (2009) 80-86.

[68] S. Tokumoto, K. Mori, N. Higo, K. Sugibayashi, Effect of electroporation on the electroosmosis across hairless mouse skin in vitro. *J. Control. Release* **105**(3) (2005) 296-304.

[69] C. Lombry, N. Dujardin, V.R. Préat, Transdermal delivery of macromolecules using skin electroporation. *Pharm. Res.* **17**(1) (2000) 32-37.

[70] Y. Tokudome, K. Sugibayashi, The effects of calcium chloride and sodium chloride on the electroporation-mediated skin permeation of fluorescein isothiocyanate (FITC)-dextrans in vitro. *Biol. Pharm. Bull.* **26**(10) (2003) 1508-1510.

[71] M. Bouclier, A. Jomard, N. Kail, B. Shroot, C. Hensby, Induction of ornithine decarboxylase activity in hairless rat epidermis as a pharmacological model: validation of the animal model. *Lab. Anim.* **21**(3) (1987) 233-240.

[72] T.E. Zewert, U.F. Pliquett, R. Vanbever, R. Langer, J.C. Weaver, Creation of transdermal pathways for macromolecule transport by skin electroporation and a low toxicity, pathway-enlarging molecule. *Bioelectrochem. Bioenerg.* **49**(1) (1999) 11-20.

[73] A.R. Denet, R. Vanbever, V. Preat, Skin electroporation for transdermal and topical delivery. *Adv. Drug Deliv. Rev.* **56**(5) (2004) 659-674.

[74] M.R. Prausnitz, The effects of electric current applied to skin: A review for transdermal drug delivery. *Adv. Drug Deliv. Rev.* **18**(1996) 395-425.

[75] U.F. Pliquett, T.E. Zewert, T. Chen, R. Langer, J.C. Weaver, Imaging of fluorescent molecule and small ion transport through human stratum corneum during high voltage pulsing: localized transport regions are involved. *Biophys. Chem.* **58**(1-2) (1996) 185-204.

[76] A. Sharma, M. Kara, F.R. Smith, T.R. Krishinan, Transdermal Drug Delivery Using Electroporation. I. Factors Influencing In Vitro Delivery of Terazosin Hydrochloride in Hairless Rats. *J. Pharm. Sci.* **89**(4) (1999) 528-535.

[77] S.M. Becker, A.V. Kuznetsov, Thermal damage reduction associated with in vivo skin electroporation: A numerical investigation justifying aggressive pre-cooling. *Int. J. Heat Mass Transf.* **50**(2007) 105-116.

[78] S. Messager, A.C. Hann, P.A. Goddard, P.W. Dettmar, J.Y. Maillard, Assessment of skin viability: is it necessary to use different methodologies? *Skin Res. Technol.* **9**(4) (2003) 321-330.

[79] D.B. Bommannan, J. Tamada, L. Leung, R.O. Potts, Effect of electroporation on transdermal iontophoretic delivery of luteinizing hormone releasing hormone (LHRH)

in vitro. *Pharm. Res.* **11**(12) (1994) 1809-1814.

[80] S.L. Chang, G.A. Hofmann, L. Zhang, L.J. Deftos, A.K. Banga, The effect of electroporation on iontophoretic transdermal delivery of calcium regulating hormones. *J. Control. Release* **66**(2-3) (2000) 127-133.

[81] A.R. Denet, B. Ucakar, V. Preat, Transdermal delivery of timolol and atenolol using electroporation and iontophoresis in combination: a mechanistic approach. *Pharm. Res.* **20**(12) (2003) 1946-1951.

[82] U.F. Pliquett, C.A. Gusbeth, J.C. Weaver, Non-linearity of molecular transport through human skin due to electric stimulus. *J. Control. Release* **68**(3) (2000) 373-386.

[83] L. Le, J. Kost, S. Mitragotri, Combined effect of low-frequency ultrasound and iontophoresis: applications for transdermal heparin delivery. *Pharm. Res.* **17**(9) (2000) 1151-1154.

[84] S. Tokumoto, K. Mori, N. Higo, K. Sugibayashi, Effect of electroporation on the electroosmosis across hairless mouse skin in vitro. *J. Control. Release* **105**(3) (2005) 296-304.

[85] R. Vanbever, U.F. Pliquett, V. Preat, J.C. Weaver, Comparison of the effects of short, high-voltage and long, medium-voltage pulses on skin electrical and transport properties. *J. Control. Release* **60**(1) (1999) 35-47.

[86] K. Mori, T. Hasegawa, S. Sato, K. Sugibayashi, Effect of electric field on the enhanced skin permeation of drugs by electroporation. *J. Control. Release* **90**(2) (2003) 171-179.

[87] K. Sugibayashi, M. Yoshida, K. Mori, T. Watanabe, T. Hasegawa, Electric field analysis on the improved skin concentration of benzoate by electroporation. *Int. J. Pharm.* **219**(1-2) (2001) 107-112.

[88] S.M. Bal, J. Caussin, S. Pavel, J.A. Bouwstra, In vivo assessment of safety of microneedle arrays in human skin. *Eur. J. Pharm. Sci.* **35**(3) (2008) 193-202.

[89] K. Yan, H. Todo, K. Sugibayashi, Transdermal drug delivery by in-skin electroporation using a microneedle array. *Int. J. Pharm.* **397**(1-2) (2010) 77-83.

[90] U. Pliquett, C. Gusbeth, R. Nuccitelli, A propagating heat wave model of skin electroporation. *J. Theor. Biol.* **251**(2) (2008) 195-201.

[91] M. Larsson, W. Steenbergen, T. Stromberg, Influence of optical properties and fiber separation on laser doppler flowmetry. *J. Biomed. Opt.* **7**(2) (2002) 236-243.